The Clebsch–Gordan coefficients of the three-dimensional Lorentz algebra in the parabolic basis[a)]

Debabrata Basu[b)] and Kurt Bernardo Wolf
Instituto de Investigaciones en Matemáticas Aplicadas y en Sistemas (IIMAS), Universidad Nacional Autónoma de México, México 20 D. F., Mexico

(Received 28 September 1981; accepted for publication 23 December 1981)

Starting from the oscillator representation of the three-dimensional Lorentz algebra so(2,1), we build a Lie algebra of second-order differential operators which realizes all series of self-adjoint irreducible representations. The choice of the common self-adjoint extension over a two-chart function space determines whether they lead to single- or multivalued representations over the corresponding Lie group. The diagonal operator defining the basis is the parabolic subgroup generator. The direct product of two such algebras allows for the calculation of all Clebsch–Gordan coefficients explicitly, as solutions of Schrödinger equations for Pöschl–Teller potentials over one ($\mathscr{D}\times\mathscr{D}$), two ($\mathscr{D}\times\mathscr{C}$), or three ($\mathscr{C}\times\mathscr{C}$) charts. All coefficients are given in terms of up to two ${}_2F_1$ hypergeometric functions.

PACS numbers: 02.20.Sv

I. INTRODUCTION

The reduction of the direct product of two self-adjoint irreducible representations (SAIR's) of a Lie algebra into a direct sum of SAIR's of the same algebra is a problem of fundamental importance in applications of both compact and noncompact algebras and groups in physics. In view of the Wigner–Eckart theorem, the keystone of many practical calculations, it can be considered among the central problems, on par with the classification and explicit construction of the SAIR matrices or integral kernels.

After the classification and construction of the unitary irreducible representations (UIR's) of the three-dimensional Lorentz group SO(2,1) was solved by Bargmann,[1] many authors considered the Clebsch–Gordan (CG) problem for the corresponding algebra so(2,1). This problem consists of two parts. The first is the determination of the CG series, and the second is the explicit evaluation of the Clebsch–Gordan coefficients (CGC's) which effect the reduction. The SAIR's of so(2,1) can be classified—following Bargmann's nomenclature—into discrete ($\mathscr{D}$) and continuous ($\mathscr{C}$) series, which in turn divide into various types: (positive and negative) discrete $D^{\pm}_{k}$, nonexceptional and exceptional continuous C^{ϵ}_{q} whose precise definition is given in the Appendix. The essentially distinct direct products to be considered are $D^{+}\times D^{+}$, $D^{+}\times D^{-}$, $\mathscr{D}\times\mathscr{C}$, and $\mathscr{C}\times\mathscr{C}$. The CG series for these four couplings changes nontrivially as one goes from case to case (they are listed in the Appendix). This structure, nevertheless, has an intrinsic meaning in that it does not depend on the particular choice of basis in the Hilbert space of representations. The CGC's, on the other hand, are manifestly basis-dependent.

The Clebsch–Gordan problem for so(2,1) was investigated by Pukánszky,[2] Holman and Biedenharn,[3,4] Ferretti and Verde,[5] Wang,[6] and by Mukunda and Radhakrishnan[7] among others.[8] Pukánszky confined his attention essentially to the structure of the CG series for the $\mathscr{C}\times\mathscr{C}$ couplings. He started from the realization of the UIR's of SO(2,1) in the Hilbert space of functions on the unit circle, decomposing their tensor product and restricting attention to the subspace for which the total magnetic quantum number is zero. He did not attempt the problem of explicit evaluation of the CGC's and of their orthonormalization. This aspect of the problem was considered by Holman and Biedenharn (HB) and by Wang. HB based their investigation on the fundamental recurrence relation satisfied by the CGC's in the compact subgroup basis. Their first paper[3] was mainly concerned with the coupling of two discrete-series representations and analytic continuation properties with the rotation group CGC's, while all coupling cases were considered in their second paper[4] in the same basis. The results are given in terms of ${}_3F_2$ generalized hypergeometric functions of unit argument. The problem is mathematically much simpler when the SAIR's coupled belong to one of the discrete series; the CGC's [in the elliptic so(2) basis] for this special coupling problem are well known, and their symmetry properties have been thoroughly investigated. The complexity of the problem progressively increases as one goes from the discrete to the continuous nonexceptional and to the exceptional types of SAIR's. Nonnormalized CGC's for the coupling of the continuous nonexceptional UIR's were derived by Ferretti and Verde.[5] Their method was based on the formula

$$d^{k_1}_{m_1'm_1}(z)d^{k_2}_{m_2'm_2}(z) = \mathop{\mathrm{S}}_{k} C\begin{pmatrix}k_1, & k_2; & k\\ m_1, & m_2; & m\end{pmatrix} C\begin{pmatrix}k_1, & k_2; & k\\ m_1', & m_2'; & m'\end{pmatrix}^{*} d^{k}_{m_1'+m_2',m_1+m_2}(z), \tag{1.1}$$

where the d's are Bargmann's SO(2,1) UIR functions,[1] the C's are the CGC's, and S denotes the summation over discrete and integration over the continuous series. The expansion is obtained by the use of the Burchnall–Chaundy[9] formula, followed by a Sommerfeld–Watson transformation.

[a)] Work performed under financial assistance from CONACYT, Project ICCBIND 790370.

[b)] On leave from Dept. of Physics, Indian Institute of Technology, Kharagpur, India.

 0022-2488/83/030478-23$02.50

The results of Ferretti and Verde formed the starting point of the investigations by Wang,[6] who attempted to orthonormalize the CGC's by adopting a summation prescription originally due to HB. [It should be noted that this apparently leads to a divergent expression in one case: Eq. (2.46) of Ref. 4 for $\mathscr{C}\times\mathscr{C}$; the convergence criterion for ${}_3F_2(1)$ is not fulfilled.]

All these authors used the maximal compact subalgebra basis for the evaluation of the CGC's. More recently, Mukunda and Radhakrishnan[7] have made a departure from this in evaluating the CG coefficients in the noncompact hyperbolic so(1,1) basis. A very attractive feature of their treatment is that they relate the CGC's with the UIR's of SO(4), SO(3,1), and SO(2,2) in various compact and noncompact bases, some of which require evaluation, and followed by Mellin transformation and composition. [Equations (5.4a), (5.4b), and (5.8c) for $\mathscr{D}\times\mathscr{C}$ in Ref. 7c and (5.8b) for $\mathscr{C}\times\mathscr{C}$ in Ref. 7d also exhibit divergent ${}_3F_2(1)$'s. These results cannot therefore be regarded as final.]

The purpose of the present paper is to give a comprehensive evaluation of the Clebsch–Gordan coefficients in the parabolic (or horocyclic) iso(1) basis, for all couplings. With the choice of this new basis the CGC's have especially simple forms: They are in general expressible in terms of single, real Gauss ${}_2F_1$ hypergeometric functions, or at most a sum of two of them

The plan of this article is as follows. We start in Sec. II reviewing the oscillator realization of the so(2,1) algebra[10] [Eqs. (2.1)]. This realization is unique in that it consists of second-order differential operators, rather than first-order ones, as Lie algebras of transformation groups do; as a result, the operator domain problem is not as trivial as it may appear at first sight. On $\mathscr{L}^2(R)$, the SAIR of this algebra exponentiates to an integral-transform UIR of the metaplectic group[11] Mp $(2,R)$ [the fourfold covering of SO(2,1) or twofold covering of $SU(1,1)\approx SL(2,R)\approx Sp(2,R)$]. These are the linear canonical transforms.[12–14] In this paper we remain within the Lie algebra, however, so Secs. III and IV are devoted to building—through coupling—the SAIR's of the discrete and continuous nonexceptional series. This construction is important, even though it yields only the SAIR's of so(2,1) which exponentiate to single-valued UIR's of $Sp(2,R)$ and does not include the exceptional continuous series, since it leads us to the consideration of $\mathscr{L}^2$-Hilbert spaces of functions on a space $\mathscr{S}=\{-1,+1\}\times R^+$, i.e., containing two R^+ charts (which can also be viewed as two-component vectors[14,15]). There, the so(2,1) generators have the form (4.14). In the $\mathscr{C}$-series they are Schrödinger Hamiltonians corresponding to harmonic or repulsive oscillators with a strong centripedal singularity at the origin. Singular potentials on a two-chart space is a feature not too familiar for physicists. Section V explores all common self-adjoint extensions of this algebra of operators in $\mathscr{L}^2(\mathscr{S})$, leading to all SAIR series of so(2,1), $\mathscr{D}$ as well as $\mathscr{C}$.

The distinct usefulness of the parabolic basis is that the defining subalgebra generator $J_-=J_0-J_1$ on $\mathscr{S}$ is $\sigma r^2/2$, $\sigma=\pm 1$ [Eq. (4.14e)], and its eigenfunctions are thus Dirac δ's on $\mathscr{S}$. The general CG problem of coupling two SAIR's is thus set up in Sec. VI as an eigenbasis problem in $\mathscr{L}^2(\mathscr{S}^2)$ where the coupled-basis Casimir operator is diagonal. The space $\mathscr{S}^2$ is parametrized into six charts, up to three of which are needed for any one coupling. In every chart, the Casimir operator eigenvalue equation takes the form of the Schrödinger equation for a Pöschl–Teller potential[16,17] of the first or of the second kind, with strong or weak barriers or wells at the end points. The solutions of these equations are given in terms of Gauss ${}_2F_1$ hypergeometric functions. When a coupling requires more than one chart, a cancellation of the boundary Wronskians must take place. The particulars of the computation of the CGC's for $D^+\times D^+$, $D^+\times D^-$, $\mathscr{D}\times\mathscr{C}$, and $\mathscr{C}\times\mathscr{C}$ couplings are given in Secs. VII, VIII, IX, and X, respectively. We omit inessential calculational labor, but give some details on the construction of multichart Kronecker- and Dirac-orthonormal solutions to the Casimir operator eigenfunction problem, which in Secs. IX and X has both point and continuous spectrum. Section XI, finally, presents some concluding remarks and offers some directions for further work.

Some convenient notational minutae: We denote by R the real line, by R^+ the interval $[0,\infty)$, by Z the integers, and by Z^+ the subset $\{0,1,2,\cdots\}$. In order to write compactly that some SAIR index k belongs to the continuous nonexceptional representation [i.e., $k=(1+i\kappa)/2$, $\kappa\in R^+$], we write $k\in C$, and to the continuous exceptional type [i.e., $k=(1+\kappa)/2$, $\kappa\in(0,1)$] we write $k\in E$. It is thereby understood that the multivaluation index ϵ (see the Appendix) ranges in the appropriate intervals, and $k\in\mathscr{C}$ is meant to stand for (k,ϵ). Similarly, $k\in D^\pm$ means that the representation k belongs to the upper- or lower-bound discrete series. If the latter distinction in unimportant, we write $k\in\mathscr{D}$ and imply $(k,\pm)$ when writing k. Effecting the product of a D^+ and C representations, and extracting from the direct sum a coupled D^+ representation is indicated as $D^+\times C\to D^+$. D^+_ϱ stands for the lower-bound oscillator representation $D^+_{1/4}+D^+_{3/4}$. The Clebsch–Gordan coefficients in the first two sections are denoted as in (3.15) or (4.10); later, as the need for full generality arises, they are denoted as in (6.19).

II. THE OSCILLATOR REPRESENTATION

2.1: Consider the three formal differential operators in the real variable $x\in R$,

$$J^\varrho_1=\frac{1}{4}\left(-\frac{d^2}{dx^2}-x^2\right), \tag{2.1a}$$

$$J^\varrho_2=-\frac{i}{4}\left(x\frac{d}{dx}+\frac{1}{2}\right), \tag{2.1b}$$

$$J^\varrho_0=\frac{1}{4}\left(-\frac{d^2}{dx^2}+x^2\right), \tag{2.1c}$$

and their linear combinations

$$J^\varrho_+=J^\varrho_0+J^\varrho_1=-\frac{1}{2}\frac{d^2}{dx^2}, \tag{2.1d}$$

$$J^\varrho_-=J^\varrho_0-J^\varrho_1=\tfrac{1}{2}x^2, \tag{2.1e}$$

among which we find the Schrödinger Hamiltonians for the harmonic (2.1c) and repulsive (2.1a) oscillators and the free particle (2.1d). The set of operators (2.1) exhibits the commutation relations of the generators of so(2,1):

$$[J_1, J_2] = -iJ_0, \quad [J_0, J_1] = iJ_2, \quad [J_2, J_0] = iJ_1. \tag{2.1f}$$

The Casimir operator is a multiple of the identity:

$$Q^{\sigma} = (J_1^{\sigma})^2 + (J_2^{\sigma})^2 - (J_0^{\sigma})^2 = \tfrac{3}{16}\mathbf{1}. \tag{2.1g}$$

The generators (2.1) are also known to have a unique common self-adjoint extension[18] in the Hilbert space $\mathcal{L}^2(R)$, whose defining inner product is

$$(f,g)_R = \int_{-\infty}^{\infty} dx\, f(x)^* g(x). \tag{2.2}$$

2.2: The realization (2.1) of so(2,1) in $\mathcal{L}^2(R)$ is called the positive oscillator[10] representation D^{+}_{σ}. It is not an irreducible representation, but in fact consists of the direct sum of two SAIR's, $D^{+}_{1/4}$ and $D^{+}_{3/4}$. The Bargmann eigenvalue of (2.2), $q = k(1-k)$, has the value $\frac{3}{16}$ for both. In order to distinguish between the two direct summands, we may use the eigenvalues ι of the inversion operator $I: f(x) = f(-x) = \iota f(x)$. The even (odd) harmonic oscillator wavefunctions belong to the eigenvalues $\mu = \epsilon + n$, $n \in Z^{+}$, $\epsilon = (2-\iota)/4$, under J_0^{σ}, for $k = \frac{1}{4}$ ($k = \frac{3}{4}$). These functions form a complete orthonormal basis for $\mathcal{L}^2_{\iota}(R)$, the space of $\mathcal{L}^2(R)$ functions with that parity. They also define common self-adjoint extensions of the algebra operators (2.1) in $\mathcal{L}^2(R^{+})$ with boundary conditions given by the vanishing of the function or of its derivative, respectively, at the origin.

2.3: The operator whose eigenbasis we want to exploit in this paper is J_-, given by (2.1e). Such a Dirac-orthonormal generalized eigenbasis, complete for $\mathcal{L}^2(R)$, is $\{\delta(x-\rho), \rho \in R\}$, with eigenvalues $\rho^2/2 \in R^{+}$. The spectrum of J^{σ}_{-} thus covers R^{+} twice. The decomposition according to the irreducible components of D^{+}_{σ} is easily accomplished through demanding definite parity. Thus

$$\psi^{1/4}_{\rho}(x) = (2\rho)^{-1/2}[\delta(x-\rho) + \delta(x+\rho)], \tag{2.3a}$$

$$\psi^{3/4}_{\rho}(x) = (2\rho)^{-1/2}[\delta(x-\rho) - \delta(x+\rho)], \quad x \in R, \ \rho \in R^{+}, \tag{2.3b}$$

constitute Dirac bases for even ($\iota = +1$) and odd ($\iota = -1$) functions, respectively. They have been chosen orthonormal in the Dirac sense:

$$(\psi^k_{\rho_1}, \psi^k_{\rho_2})_R = \rho_1^{-1}\delta(\rho_1 - \rho_2) = \delta(\rho_1^2/2 - \rho_2^2/2), \tag{2.4a}$$

for k either $\frac{1}{4}$ or $\frac{3}{4}$. Orthogonality in the upper index also holds, but will not be used. They are complete in the sense

$$\int_0^{\infty} d(\rho^2/2)\psi^k_{\rho}(x)^* \psi^k_{\rho}(x') = \delta(x - x'), \tag{2.4b}$$

where the right-hand side is the reproducing kernel in the space of the corresponding parity ι. The operators (2.1) with these domains will be indicated, respectively, by $J^{1/4}_{\alpha}$ and $J^{3/4}_{\alpha}$ ($\alpha = 1,2,0,+,-$). In particular, the generalized spectrum of J^{k}_{-}, $k = \frac{1}{4}$ or $\frac{3}{4}$, is now simple: A single eigenfunction $\psi^k_{\rho}(x)$ corresponds to each eigenvalue $\rho^2/2 \in R^{+}$, $\rho \in R^{+}$.

2.4: The negative oscillator representation D^{-}_{σ} of so(2,1) is obtained from the D^{+}_{σ} representation seen above by means of the outer automorphism of the algebra $A: J^{\sigma}_{\alpha} \mapsto J^{\sigma}_{\alpha}{}^{-}$, where

$$J_1^{k-} = -J_1^k, \quad J_2^{k-} = J_2^k,$$
$$J_0^{k-} = -J_0^k, \quad J_{\pm}^{k-} = -J_{\pm}^k, \tag{2.5a}$$

for $k = \sigma$, or $\frac{1}{4}, \frac{3}{4}$ after decomposition into its irreducible components. The Casimir operator does not distinguish between positive and negative representations:

$$Q^{k-} = Q^k = Q^{\sigma} = \tfrac{3}{16}\mathbf{1} \quad (k = \tfrac{1}{4}, \tfrac{3}{4}). \tag{2.5b}$$

In this way we produce the $D^{-}_{1/4}$ and $D^{-}_{3/4}$ SAIR's out of the D^{+}_{k} ones. The spectrum of J^k_0 changes sign under the automorphism A, and so does the spectrum of J^{k}_{-} which is now $-\rho^2/2 \in R^{-}, \rho \in R^{+}$, still simple, and with generalized eigenfunctions formally identical to (2.3a) and (2.3b).

III. THE OSCILLATOR COUPLING TO THE DISCRETE SERIES

In this section we consider the direct product of two irreducible components of the oscillator representation, decomposed into a direct sum of SAIR's D^{+}_{k} belonging to the positive discrete series.

3.1: Consider the two sets of so(2,1) generators, mutually commuting, given as in (2.1), in terms of two independent variables x_j, $j = 1,2$, and denote them by $J^{k_j}_{(j)\alpha}$ ($j = 1,2$, respectively, $\alpha = 1,2,0,+,-$; $k_j = \frac{1}{4}$ in the space $\mathcal{L}^2_{+1}(R)$ of even functions in x_j, and $k_j = \frac{3}{4}$ in the space $\mathcal{L}^2_{-1}(R)$ of odd functions in x_j). Out of these we build the two-variable operators

$$J^{k_1,k_2}_{\alpha} = J^{k_1}_{(1)\alpha} + J^{k_2}_{(2)\alpha}. \tag{3.1}$$

These operators will have a correspondingly unique self-adjoint extension in the Hilbert space $\mathcal{L}^2_{\iota_1,\iota_2}(R^2) = \mathcal{L}^2_{\iota_1}(R) \times \mathcal{L}^2_{\iota_2}(R)$, with inner product

$$(f,g)_{R^2} = \int_{-\infty}^{\infty} dx_1 \int_{-\infty}^{\infty} dx_2 f(x_1,x_2)^* g(x_1,x_2) = \int_0^{\infty} r\,dr \int_{-\pi}^{\pi} d\theta\, f[r,\theta]^* g[r,\theta], \tag{3.2}$$

where we have introduced polar coordinates in the plane:

$$x_1 = r\cos\theta, \quad x_2 = r\sin\theta, \quad r \in R^{+}, \quad \theta \equiv \theta \pmod{2\pi}. \tag{3.3}$$

All functions $f(x_1,x_2)$ in the domain of J^{k_1,k_2}_{α} have parity ι_j under inversions $x_j \leftrightarrow -x_j$ when $k_j = \frac{1}{4}, \frac{3}{4}$ as above. The Casimir operator (2.2) corresponding to the factor operator set $J^{k_j}_{(j)\alpha}$ will be denoted by $Q^{k_j}_{(j)}$, and that of the coupled set J^{k_1,k_2}_{α} will be denoted by Q^{k_1,k_2}.

3.2: We shall define the product states as the generalized eigenfunctions of the four commuting operators

$$Q^{k_1}_{(1)}, \quad Q^{k_2}_{(2)}, \quad J^{k_1}_{(1)-}, \quad J^{k_2}_{(2)-}. \tag{3.4}$$

The first two operators are here identically $\frac{3}{16}\mathbf{1}$, while the second pair determine the product states to be

$$\psi^{k_1,k_2}_{\rho_1,\rho_2}(x_1,x_2) = \psi^{k_1}_{\rho_1}(x_1)\psi^{k_2}_{\rho_2}(x_2) \tag{3.5}$$

in terms of (2.3), with eigenvalues $\rho_1^2/2$ and $\rho_2^2/2$, respectively. From (2.4) they are Dirac-orthonormal and complete:

$$(\psi^{k_1,k_2}_{\rho_1,\rho_2}, \psi^{k_1,k_2}_{\rho_1',\rho_2'})_{R^2} = \delta(\rho_1^2/2 - \rho_1'^2/2)\delta(\rho_2^2/2 - \rho_2'^2/2). \tag{3.6}$$

Orthogonality for the indices k_1, k_2 also holds, but will not be

needed.

3.3: The coupled states are defined as the generalized eigenfunctions of the four commuting operators

$$Q_{(1)}^{k_1}, \quad Q_{(2)}^{k_2}, \quad Q^{k_1,k_2}, \quad J_{-}^{k_1,k_2}, \tag{3.7}$$

in the same space $\mathscr{L}^2_{\iota_1,\iota_2}(R^2)$. Again, the first two operators are $\frac{3}{16}\mathbf{1}$ while the last one may be written in terms of the polar coordinates (3.3) as

$$J_{-}^{k_1,k_2} = J_{(1)-}^{k_1} + J_{(2)-}^{k_2} = x_1^2/2 + x_2^2/2 = r^2/2. \tag{3.8}$$

The generalized eigenfunctions of (3.7) will therefore include a factor $\delta(r^2/2 - \rho^2/2)$ so that they be Dirac-orthogonal eigenfunctions of $J_{-}^{k_1,k_2}$ under (3.2), with eigenvalue $\rho^2/2$. This, in turn, will produce a selection rule $\rho_1^2/2 + \rho_2^2/2 = \rho^2/2$ in the CGC. Finally, the coupled Casimir operator Q^{k_1,k_2} may be written in terms of (2.1), (2.2), (3.1), and (3.3) as

$$\begin{aligned} Q^{k_1,k_2} &= Q_{(1)}^{k_1} + Q_{(2)}^{k_2} + 2(J_{(1)1}^{k_1} J_{(2)1}^{k_2} + J_{(1)2}^{k_1} J_{(2)2}^{k_2} - J_{(1)0}^{k_1} J_{(2)0}^{k_2}) \\ &= \frac{1}{4} + \frac{1}{4}\frac{\partial^2}{\partial\theta^2}. \end{aligned} \tag{3.9}$$

Since the spectrum of $\partial^2/\partial\theta^2$ on $\mathscr{L}^2(S_1)$ (the Hilbert space of square-integrable functions on the circle) is negative (and discrete), we are assured of having coupled representations belonging to the discrete series. Whereas the product states separate in Cartesian coordinates, the coupled states separate in polar coordinates, and consequently may be written as

$$\Psi_{k,\rho}^{k_1,k_2}(r,\theta) = \delta(r^2/2 - \rho^2/2) F_k^{k_1,k_2}(\theta), \tag{3.10}$$

with $F_k^{k_1,k_2}(\theta)$ a solution of

$$Q^{k_1,k_2} F_k^{k_1,k_2}(\theta) = k(1-k) F_k^{k_1,k_2}(\theta), \tag{3.11}$$

properly normalized in $\mathscr{L}^2(S_1)$ and such that it satisfies the parity properties of the space of functions.

The θ-dependent factors $F_k^{k_1,k_2}(\theta)$ of the coupled states must be of the form $\exp(im\theta)$ with m integer [so that it is periodic] and $k(1-k) = (1-m^2)/4$, i.e., $k = (1 + |m|)/2$. As functions of $\theta = \arctan(x_2/x_1)$ they must be even (odd) under $x_1 \leftrightarrow -x_1$, $\theta \leftrightarrow \pi - \theta$ when $k_1 = \frac{1}{4}$ ($k_1 = \frac{3}{4}$) and even (odd) under $x_2 \leftrightarrow -x_2$, $\theta \leftrightarrow -\theta$. These requirements are met, as a selection rule, when performing the inner product with the product states (3.5), but it is illuminating to impose them on the coupled state. What they imply is that: (i) The $(k_1,k_2) = (\frac{1}{4},\frac{1}{4})$ coupling may only contain $\cos m\theta$ with m even; (ii) the $(\frac{3}{4},\frac{3}{4})$ coupling, only $\sin m\theta$ with m even (excluding thus $m = 0$); (iii) the $(\frac{1}{4},\frac{3}{4})$ and $(\frac{3}{4},\frac{1}{4})$ couplings, only $\sin m\theta$ and $\cos m\theta$, respectively, with m odd. An elementary analysis involving the J_0 eigenvalues will confirm these selection rules. The choice of phases for the product and coupled states has been made out of simplicity.

3.4: The normalized coupled states are thus built out of (3.10) with

$$F_k^{1/4,1/4}(\theta) = \begin{cases} (2\pi)^{-1/2}, & k = \frac{1}{2}, \\ \pi^{-1/2}\cos(2k-1)\theta, & k = \frac{3}{2},\frac{5}{2},\cdots, \end{cases} \tag{3.12a}$$

$$F_k^{3/4,3/4}(\theta) = \pi^{-1/2}\sin(2k-1)\theta, \quad k = \tfrac{3}{2},\tfrac{5}{2},\cdots, \tag{3.12b}$$

$$F_k^{1/4,3/4}(\theta) = \pi^{-1/2}\sin(2k-1)\theta, \quad k = 1,2,\cdots, \tag{3.12c}$$

$$F_k^{3/4,1/4}(\theta) = \pi^{-1/2}\cos(2k-1)\theta, \quad k = 1,2,\cdots, \tag{3.12d}$$

and satisfy

$$(\Psi_{k,\rho}^{k_1,k_2}, \Psi_{k',\rho'}^{k_1,k_2})_{R^2} = \delta_{k,k'}\delta(\rho^2/2 - \rho'^2/2). \tag{3.13}$$

Again, orthogonality in k_1 and k_2 indices is present but will not be used.

3.5: The normalization coefficient $\pi^{-1/2}$ in (3.12) is trivial to obtain from integral tables or through a number of elementary analyses. We would like to present here, however, the method which will be used, especially in Secs. IX and X, for more complicated point-spectrum eigenfunctions. Write $F_k(\theta) = c_k f_k(\theta)$ and $F_l(\theta) = c_l f_l(\theta)$, eigenfunctions of Q in (3.9) with eigenvalues $k(1-k)$ and $l(1-l)$, respectively, $f_k(\theta) = \sin(2k-1)\theta$ or $\cos(2k-1)\theta$, and c_k to be determined. Then, the integral over any interval $(a,b) \subset R$ may be put, through multiplying the eigenvalue equation of f_k^* by f_l and vice versa, and taking the difference, in terms of the boundary Wronskians as

$$\begin{aligned} \int_a^b d\theta f_k^* f_l &= [4(l+k-1)(l-k)]^{-1} W(f_k^*, f_l)\,|_a^b \\ &= [4(l+k-1)(l-k)]^{-1}[f_k^{*\prime} f_l - f_k^* f_l']\,|_b^a, \end{aligned} \tag{3.14a}$$

where the prime indicates differentiation with respect to the argument θ. The boundary term on the right-hand side vanishes when $b - a = 2\pi$ and $k = l +$ integer, assuring the orthogonality of any eigenfunction pair. Now, Eq. (3.14a) is true even when f_l (and/or f_k) is not a periodic function in θ under the period $b - a$, i.e., when $2l - 1$ is not an integer. For the normalization problem at hand, we may choose for a a point where the boundary term is zero, such as $a = 0$ and for b some other point where the term is easily evaluated. We thus write

$$\begin{aligned} \int_0^{2\pi} d\theta\, |f_k(\theta)|^2 &= 2\lim_{l\to k}\int_0^{\pi} d\theta f_k^*(\theta) f_l(\theta) \\ &= [2(2k-1)]^{-1}\lim_{(l\to k)}(l-k)^{-1} W(f_k^*, f_l)|_{\theta=\pi} \\ &= [2(2k-1)]^{-1}\frac{\partial}{\partial l} W(f_k^*, f_l)\,|_{\theta=\pi, l=k}. \end{aligned} \tag{3.14b}$$

In the cases exemplified here, the limits and valuations may be manifestly exchanged, and the result is π; it follows that $c_k = \pi^{-1/2}$, as given in (3.12). This method will be used when f_k and f_l are given hypergeometric functions, whose normalization constants are not easily evaluated by other means.

3.6: The inner products between the product and coupled states constitute the standard definition of the Clebsch–Gordan coefficients:

$$\begin{aligned} C\begin{pmatrix} k_1,k_2;k \\ \rho_1,\rho_2;\rho \end{pmatrix} &= (\psi_{\rho_1,\rho_2}^{k_1,k_2}, \Psi_{k,\rho}^{k_1,k_2})_{R^2} \\ &= 2(\rho_1\rho_2)^{-1/2}\int_0^{\pi/2} d\theta\, \delta(\rho\cos\theta - \rho_1) \\ &\quad \times \delta(\rho\sin\theta - \rho_2) F_k^{k_1,k_2}(\theta) \\ &= 2(\rho_1\rho_2)^{-1/2}\delta(\rho_1^2/2 + \rho_2^2/2 - \rho^2/2) \\ &\quad \times F_k^{k_1,k_2}(\arctan(\rho_2/\rho_1)). \end{aligned} \tag{3.15}$$

We have used the matching symmetry properties in θ of the product and coupled states to reduce the θ-integration to the first quadrant and finally express the results in terms of the solutions (3.12) to (3.11).

Noting that

$$\arctan(\rho_2/\rho_1) = \arcsin(\rho_2/\rho) = \arccos(\rho_1/\rho), \quad (3.16)$$

we can write the expressions in terms of Chebyshev polynomials of the first and second kinds (Ref. 19, Eq. 22.3.15). The CGC for the $D_{\rho}^{+} \times D_{\rho}^{+} \to D_{k}^{+}$ couplings are thus

$$C\begin{pmatrix} \frac{1}{4} & \frac{1}{4} & \frac{1}{2} \\ \rho_1 & \rho_2 & \rho \end{pmatrix} = \delta(\rho_1^2/2 + \rho_2^2/2 - \rho^2/2)(\tfrac{1}{2}\pi\rho_1\rho_2)^{-1/2}, \quad (3.17a)$$

$$C\begin{pmatrix} \frac{1}{4} & \frac{1}{4} & k \\ \rho_1 & \rho_2 & \rho \end{pmatrix} = \delta(\rho_1^2/2 + \rho_2^2/2 - \rho^2/2)\pi^{-1/2}\rho_1^{-1/2}\rho_2^{-1/2} \times T_{2k-1}(\rho_1/\rho), \quad k = \tfrac{3}{2},\tfrac{5}{2},\cdots, \quad (3.17b)$$

$$C\begin{pmatrix} \frac{3}{4} & \frac{3}{4} & k \\ \rho_1 & \rho_2 & \rho \end{pmatrix} = \delta(\rho_1^2/2 + \rho_2^2/2 - \rho^2/2)2\pi^{-1/2}\rho_1^{-1/2}\rho_2^{1/2}\rho^{-1} \times U_{2k-2}(\rho_1/\rho), \quad k = \tfrac{3}{2},\tfrac{5}{2},\cdots, \quad (3.17c)$$

$$C\begin{pmatrix} \frac{1}{4} & \frac{3}{4} & k \\ \rho_1 & \rho_2 & \rho \end{pmatrix} = C\begin{pmatrix} \frac{3}{4} & \frac{3}{4} & k \\ \rho_1 & \rho_2 & \rho \end{pmatrix}, \quad k = 1,2,\cdots, \quad (3.17d)$$

$$C\begin{pmatrix} \frac{3}{4} & \frac{1}{4} & k \\ \rho_1 & \rho_2 & \rho \end{pmatrix} = C\begin{pmatrix} \frac{1}{4} & \frac{1}{4} & k \\ \rho_1 & \rho_2 & \rho \end{pmatrix}, \quad k = 1,2,\cdots. \quad (3.17e)$$

$$\cos(\nu \arcsin z) = F(-\nu/2,\nu/2;\tfrac{1}{2};z^2), \quad |\mathrm{Re}\, z| < 1, \quad (3.18a)$$

$$\sin(\nu \arcsin z) = \nu z(1-z^2)^{1/2}F(-\nu/2+1,\nu/2+1;\tfrac{3}{2};z^2), \quad (3.18b)$$

we can write the CGC's for $D_{\rho}^{+} \times D_{\rho}^{+} \to D_{k}^{+}$ in terms of hypergeometric functions ${}_2F_1$.

Through application of the outer automorphism A to both product and coupled states, we find the same values for the $D_{\rho}^{-} \times D_{\rho}^{-} \to D_{k}^{-}$ CGC's as those given in (3.17) with the simple changes $k \to k^{-}$. In the parabolic basis we do not have to observe the Bargmann phase convention [Ref. 1, Eqs. (6.23) and (7.10)] which introduces a factor of $(-1)^m$ to the so(2)-classified eigenbasis.

3.7: The description of the CG series and the evaluation of the coefficients, as presented in this section, could have been made also using the completeness relation of the Fourier series on $\mathscr{L}^2(S_1)$ with the proper parities, thereby expanding the product of Dirac δ's on the plane (3.5) in terms of a Dirac δ on the radius, times the limit of the Dirichlet kernel. This method has been implemented before for the integral transform group in projecting out the k-radial canonical transform[3b] belonging to the D_{k}^{+} UIR, out of the $\mathrm{Mp}(2,R) \times \mathrm{Mp}(2,R)$ oscillator integral transform UIR. Here, we have not left the algebra level. The completeness statements for the Pöschl–Teller Schrödinger equation solutions—to be seen in Secs. VI–X—are more difficult to make than those for Fourier series.

3.8: As a preparation for Secs. V–X, we now project the coupled operators (3.1) on a definite D_{k}^{+} SAIR space ($k = \frac{1}{2},1,\frac{3}{2},2,\cdots$) using the fact that in this space the coupled Casimir operator Q^{k_1,k_2} has a definite eigenvalue $k(1-k)$. We perform a similarity transformation by $r^{1/2}$ so that the resulting operator be manifestly symmetric in $\mathscr{L}^2(R^{+})$ with inner product

$$(f,g)_{R^{+}} = \int_0^\infty dr\, f(r)^* g(r). \quad (3.19)$$

Thus

$$r^{1/2}\left(\frac{\partial^2}{\partial x_1^2} + \frac{\partial^2}{\partial x_2^2}\right)r^{-1/2} = r^{1/2}\left(\frac{\partial^2}{\partial r^2} + r^{-1}\frac{\partial}{\partial r} + r^{-2}[4Q^{k_1,k_2} - 1]\right)r^{-1/2} = \frac{\partial^2}{\partial r^2} - \frac{\gamma}{r^2}, \quad \gamma = (2k-1)^2 - \tfrac{1}{4} \geqslant -\tfrac{1}{4}. \quad (3.20)$$

We obtain hence for the $D_{k}^{\pm}$ SAIR

$$J_1^{k\pm} = \pm\frac{1}{4}\left(-\frac{d^2}{dr^2} + \frac{\gamma}{r^2} - r^2\right), \quad (3.21a)$$

$$J_2^{k\pm} = -\frac{i}{2}\left(r\frac{d}{dr} + \frac{1}{2}\right), \quad (3.21b)$$

$$J_0^{k\pm} = \pm\frac{1}{4}\left(-\frac{d^2}{dr^2} + \frac{\gamma}{r^2} + r^2\right), \quad (3.21c)$$

$$J_{+}^{k\pm} = J_0^{k\pm} + J_1^{k\pm} = \pm\frac{1}{2}\left(-\frac{d^2}{dr^2} + \frac{\gamma}{r^2}\right), \quad (3.21d)$$

$$J_{-}^{k\pm} = J_0^{k\pm} - J_1^{k\pm} = \pm\tfrac{1}{2}r^2, \quad (3.21e)$$

$$k = (1 + [\gamma + \tfrac{1}{4}])/2 \in \{\tfrac{1}{2},1,\tfrac{3}{2},2,\cdots\}. \quad (3.21f)$$

Of course, for $\gamma = 0$ we are formally back at (2.1), although k is from here on taking a range of values which excludes this case.

The Casimir operator of the so(2,1) algebra (3.21), calculated as in (2.2), yields here

$$Q^k = q\mathbf{1}, \quad q = k(1-k) = -\gamma/4 + \tfrac{3}{16} \leqslant -\tfrac{1}{4}. \quad (3.22)$$

In the next section we shall describe the domains where the operators (3.21) have self-adjoint extensions. Here we would only like to point out that if I_1 and I_2 are the inversion operators along the two axes, the space $\mathscr{L}^2_{\iota_1}(R) \times \mathscr{L}^2_{\iota_2}(R)$ will have eigenvalue $\iota = \iota_1\iota_2$ under the product inversion $I = I_1I_2$. Under the projection to a definite $Q^{k_1k_2}$ eigenvalue in (3.20), this information is lost. We may keep, however, the J_0-spectrum starting point $\epsilon_j = (2-\iota_j)/4$ defined in subsection 2.2, in order to associate with the domain of (3.21) the index $\epsilon = \epsilon_1 + \epsilon_2 = 1 - (\iota_1 + \iota_2)/4$. The spectrum of $J_0^{k\pm}$ will be contained in $\{\epsilon + n, n \in Z\}$. It is immediate to see that $\epsilon = 0$ when k is integer, and $\epsilon = \frac{1}{2}$ when k is half-integer. In fact, thus $\epsilon \equiv k \pmod 1$.

IV. THE OSCILLATOR COUPLING TO THE CONTINUOUS SERIES

We consider now the coupling of a positive and a negative oscillator representation, and their decomposition into a direct integral of SAIR's belonging to the nonexceptional continuous series.

4.1: Consider two sets of generators, $J_{(1)\alpha}^{k_1+}$ and $J_{(2)\alpha}^{k_2-}$, the first belonging to the $D_{k_1}^{+}$ summand ($k_1 = \frac{1}{4}$ or $\frac{3}{4}$) of the positive oscillator representation and the second set, obtained through (2.5) from the first, belonging to the $D_{k_2}^{-}$ negative oscillator representation. Out of these we now build, *vis-à-vis* (3.1), the two-variable operators

$$J_{\alpha}^{k_1,k_2} = J_{(1)\alpha}^{k_1+} + J_{(2)\alpha}^{k_1-} = J_{(1)\alpha}^{k_1} + \tau_\alpha J_{(2)\alpha}^{k_2}, \quad (4.1a)$$

$$\tau_\alpha = -1 \quad \text{for } \alpha = 1,0,+,-, \quad \tau_\alpha = 1 \quad \text{for } \alpha = 2, \quad (4.1b)$$

also self-adjoint with respect to the inner product $(\cdot,\cdot)_{R^2}$ in

(3.2), in the space of functions $\mathscr{L}^2_{\iota_1,\iota_2}(R^2) = \mathscr{L}^2_{\iota_1}(R) \times \mathscr{L}^2_{\iota_2}(R)$.

In particular, the diagonal operator $J_-^{k_1,k_2}$ is the difference, rather than the sum of $J^{k_1}_{(1)-}$ and $J^{k_2}_{(2)-}$. It is thus convenient to parametrize the R^2 plane in hyperbolic coordinates (σ,r,θ), $\sigma\in\{-1,+1\}$, $r\in R$, $\theta\in R$ given by

$$\text{for } |x_1|>|x_2|: \quad \sigma=+1, \quad x_1 = r\cosh\theta, \quad x_2 = r\sinh\theta, \tag{4.2a}$$

$$\text{for } |x_1|<|x_2|: \quad \sigma=-1, \quad x_1 = r\sinh\theta, \quad x_2 = r\cosh\theta, \tag{4.2b}$$

disregarding the cone $|x_1| = |x_2|$. (The fact that we are using in this section the letters r and θ to denote the hyperbolic radius and angle should lead to no confusion with the former section, where they stood for the polar radius and angle. The ensuing uniformity of notation—with the ranges specified—will be seen to be quite economical.) Note that each value of σ in (4.2) defines one coordinate chart, and both $\sigma=+1$ and $\sigma=-1$ charts are needed to cover R^2.

We may express, correspondingly, the $(\cdot,\cdot)_{R^2}$ inner product (3.2) through

$$(f,g)_{R^2} = \sum_{\sigma=\pm1}\int_{-\infty}^{\infty}|r|dr\int_{-\infty}^{\infty}d\theta f\{\sigma,r,\theta\}^* g\{\sigma,r,\theta\}, \tag{4.3}$$

where $f\{\sigma,r,\theta\} = f(x_1,x_2)$ uses the hyperbolic parametrization. We may think of $f(r,\theta)$ as a two-component function with components labeled by $\sigma=\pm1$ or included them—as we do here—as a coordinate.

4.2: As before, we define the product states as the generalized eigenfunctions of $Q^{k_1}_{(1)}$, $Q^{k_2}_{(2)}$, $J^{k_1}_{(1)-}$ and $J^{k_2}_{(2)-}$ in $\mathscr{L}^2_{\iota_1,\iota_2}(R^2)$ as in (3.5)–(2.3) with the difference that their eigenvalue under the latter operator will be $-\rho_2^2/2$, $\rho_2\in R^+$, instead of $+\rho_2^2/2$. When $\rho_1>\rho_2$ the product state is nonzero only over the $\sigma=+1$ chart, while when $\rho_1<\rho_2$, it is nonzero over the $\sigma=-1$ chart. The orthogonality relation (3.6) continues to hold.

4.3: The coupled states, again, are defined as the Dirac-normalized generalized eigenfunctions of $Q^{k_1}_{(1)}$, $Q^{k_2}_{(2)}$, Q^{k_1,k_2} and $J_-^{k_1,k_2}$ in $\mathscr{L}^2_{\iota_1,\iota_2}(R^2)$, as in (3.7) *et seq.*, except that we find it best to express them in terms of hyperbolic coordinates (4.2). Corresponding to (3.8), we have the coupled generator

$$J_-^{k_1,k_2} = J^{k_1}_{(1)-} - J^{k_2}_{(2)-} = x_1^2/2 - x_2^2/2 = \sigma r^2/2, \tag{4.4}$$

the change of sign due to (2.5). The essential spectrum of (4.4) thus covers R. Corresponding to (3.9), we have

$$\begin{aligned} Q^{k_1,k_2} &= Q^{k_1}_{(1)} + Q^{k_2}_{(2)} \\ &\quad + 2(-J^{k_1}_{(1)1}J^{k_2}_{(2)1} + J^{k_1}_{(1)2}J^{k_2}_{(2)2} + J^{k_1}_{(1)0}J^{k_2}_{(2)0}) \\ &= \frac{1}{4} - \frac{1}{4}\frac{\partial^2}{\partial\theta^2}. \end{aligned} \tag{4.5}$$

Since the spectrum $\partial^2/\partial\theta^2$ on $\mathscr{L}^2(R)$ is negative, we are assured of having coupled representations in the nonexceptional continuous series (the point $k=\frac{1}{2}$ will be subject to further discussion). The coupled states separate in hyperbolic coordinates and may be written as

$$\begin{aligned} \Psi^{k_1+,k_2-}_{k,\tau,\rho}(\sigma,r,\theta) &= \delta(\sigma r^2/2 - \tau\rho^2/2)E^{k_1,k_2}(\operatorname{sgn} r)F^{k_1+,k_2-}_{k,\tau}(\theta) \\ &= \delta_{\sigma,\tau}\delta(r^2/2-\rho^2/2)E^{k_1,k_2}(\operatorname{sgn} r)F^{k_1+,k_2-}_{k,\tau}(\theta), \end{aligned} \tag{4.6}$$

which is generalized eigenfunction of $J_-^{k_1,k_2}$ with eigenvalue $\tau\rho^2/2\in R$ and of Q^{k_1,k_2} with eigenvalue $k(1-k)\geqslant\frac{1}{4}$ provided (3.11) holds (with $\theta\in R$ now). This last equation for $F^{k_1+,k_2-}_{k,\tau}(\theta)$ has solutions $\exp(i\kappa\theta)$ for $\kappa\in R$, corresponding to $k(1-k) = (1+\kappa^2)/4$, i.e., $k = (1+i\kappa)/2$. The representations of the continuous series with κ and $-\kappa$ (k and $1-k$) are equivalent[1] so we shall restrict ourselves to $\kappa\in R^+$. Note that $\Psi^{k_1+,k_2-}_{k,\tau,\rho}(\sigma,r,\theta)$ is zero for $\sigma=-1$ when its eigenvalue under $J_-^{k_1,k_2}$ is positive, and is zero for $\sigma=+1$ when its eigenvalue is negative.

We still have to see it, explicitly, that the parities of the product states are the same as those of the coupled states. (i) The $(k_1,k_2) = (\frac{1}{4},\frac{1}{4})$ product states are even under $x_1\leftrightarrow -x_1$ and under $x_2\leftrightarrow -x_2$, i.e., even under $r\leftrightarrow -r$ and even under $\theta\leftrightarrow -\theta$, implying $E^{1/4,1/4}(-1)$, and that only a term $\cos k\theta$ may be present in $F^{k_1+,k_1-}_{\tau,k}(\theta)$. (ii) the $(\frac{3}{4},\frac{3}{4})$ product states are odd in both x_1 and x_2, hence even in r and odd in θ, so $E^{3/4,3/4}(-1)$ and only a term $\sin\kappa\theta$ may be present in (4.6). (iii) $(\frac{1}{4},\frac{3}{4})$ product states are even in x_1 and odd in x_2; for $\sigma=-1$ they are odd in r and even in θ. (iv) $(\frac{3}{4},\frac{1}{4})$ states, odd in x_1 and even in x_2 are, for $\sigma=+1$, odd in r and even in θ, while for $\sigma=-1$ they are odd in both r and θ. In all of these cases, the spectrum of J_0 is contained in $\{\epsilon+n,\ n\in Z\}$, $\epsilon = \epsilon_1-\epsilon_2 = (\iota_2-\iota_1)/4$.

4.4: To sum up, cases (i) and (ii) (which from the J_0 eigenvalue content we know belong to the C^0_q representations) are even functions of r, and cases (iii) and (iv) (belonging to the $C^{1/2}_q$ representations), are odd in r. We may hence write $E^{k_1,k_2}(\operatorname{sgn} r) = (\operatorname{sgn} r)^{2\epsilon}$, $\epsilon = |k_1-k_2|$, cut the range of r to R^+ and henceforth attach the index ϵ in front of the representation index $k = (1+i\kappa)/2$ to distinguish between the C^0_q and $C^{1/2}_q$ SAIR's. The inversion operator $I: f(x_1,x_2) = f(-x_1,-x_2)$ has eigenvalue $\iota = \iota_1\iota_2 = 1-4\epsilon$ in each ϵ-labeled irreducible space, but is no longer related to k, as it was in (3.23).

The coupled eigenstates are thus, explicitly,

$$\Psi^{k_1+,k_2-}_{\epsilon,k,\tau,\rho}(\sigma,r,\theta) = \delta_{\sigma,\tau}\delta(r^2/2-\rho^2/2)F^{k_1+,k_2-}_{\epsilon,k,\tau}(\theta), \tag{4.7}$$

where

$$F^{1/4+,1/4-}_{0,k,\tau}(\theta) = \pi^{-1/2}\cos\kappa\theta, \quad \kappa\geqslant 0, \tag{4.8a}$$

$$F^{3/4+,3/4-}_{0,k,\tau}(\theta) = \pi^{-1/2}\sin\kappa\theta, \quad \kappa>0, \tag{4.8b}$$

$$F^{1/4+,3/4-}_{1/2,k,+1}(\theta) = F^{3/4+,1/4-}_{1/2,k,-1}(\theta) = \pi^{-1/2}\sin\kappa\theta, \quad \kappa>0, \tag{4.8c}$$

$$F^{3/4+,1/4-}_{1/2,k,+1}(\theta) = F^{1/4+,3/4-}_{1/2,k,-1}(\theta) = \pi^{-1/2}\cos\kappa\theta, \quad \kappa\geqslant 0, \tag{4.8d}$$

which are generalized eigenfunctions—we repeat for clarity—of the coupled Q^{k_1,k_2} with eigenvalues $q = k(1-k)\geqslant\frac{1}{4}$, $k = (1+i\kappa)/2$, $\kappa\in R^+$, and form a basis for the continuous nonexceptional C^ϵ_q representation series, $\epsilon = |k_1-k_2|$, and of the coupled $J_-^{k_1,k_2}$ with eigenvalues $\tau\rho^2/2\in R$. The Dirac orthonormality condition which is the analog of (3.13) holds, with $\delta_{k,k'}$ replaced by $\delta_{\tau,\tau'}\delta(\kappa-\kappa')$.

4.5: Again, as in subsection 3.5, we would like to present a method for finding the Dirac-normalization coefficient

$\pi^{-1/2}$ present in (4.8), with the purpose of following the same line of computation in Dirac-normalizing more difficult functions in later sections. Consider $F_k(\theta)=c_k f_k(\theta)$ and $F_l(\theta)=c_l f_l(\theta)$ with $f_k(\theta)=\sin\kappa\theta$ or $\cos\kappa\theta$, $2k-1=i\kappa$, $2l-1=i\lambda$ with support on a single σ chart. Equation (3.14a), stemming from the Casimir operator equation (4.5), holds, with a change of sign obtained through replacing $4(l+k-1)(l-k)\mapsto(\lambda+\kappa)(\lambda-\kappa)$, and since the functions involved have definite parity,

$$\begin{aligned}\lim_{L\to\infty}\int_{-L}^{L} d\theta f_k(\theta)^* f_l(\theta)\\ &=2\lim_{L\to\infty}[(\lambda+\kappa)(\lambda-\kappa)]^{-1}W(f_k^*,f_l)\,|_0^L\\ &=\lim_{L\to\infty}\left[\frac{\sin(\lambda-\kappa)\theta}{\lambda-\kappa}\mp\frac{\sin(\lambda+\kappa)\theta}{\lambda+\kappa}\right]\Bigg|_{\theta=L}\\ &=\pi[\delta(\lambda-\kappa)\mp\delta(\lambda+\kappa)]=\pi\delta(\lambda-\kappa),\end{aligned}\tag{4.9}$$

the upper or lower signs holding for the sine or cosine functions. The $\mp\delta(\lambda+\kappa)$ summand may be discarded on the grounds of the range of the representation indices. The behavior at infinity, being that of the Dirichlet kernel for Fourier transforms, determines the Dirac normalization constant of (4.8) to be $\pi^{-1/2}$. The existence of a limit in the mean will also serve to find the proper linear combination coefficient for the two independent solutions of the Casimir eigenvalue equation so that they form a Dirac-orthonormal set.

4.6: The CGC, finally, is obtained as the inner product between the product and coupled states, as in (3.14). The chart which supports the four δ's in the product state is given by $\sigma=\mathrm{sgn}(\rho_1^2-\rho_2^2)=\tau$, and thus in turn yields $\theta=\mathrm{arctanh}(\rho_2/\rho_1)=\mathrm{arcsinh}(\rho_2/\rho)$ for $\sigma=+1$ and $\theta=\mathrm{arccoth}(\rho_2/\rho_1)=\mathrm{arcsinh}(\rho_1/\rho)$ for $\sigma=-1$. We thus arrive at the general expression

$$\begin{aligned}C\begin{pmatrix}k_1+,k_2-;\epsilon k\\ \rho_1,\ \rho_2\ ;\tau,\rho\end{pmatrix}&=(\psi^{k_1+,k_2-}_{\rho_1,\rho_2},\Psi^{k_1+,k_2-}_{\epsilon,k,\tau,\rho})_{R^2}\\ &=2(\rho_1\rho_2)^{-1/2}\delta(\rho_1^2/2-\rho_2^2/2-\tau\rho^2/2)\\ &\quad\times F^{k_1+,k_2-}_{\epsilon,k,\tau}(\mathrm{arctanh}[(\rho_2/\rho_1)^\tau]).\end{aligned}\tag{4.10}$$

Comparing the above expression with its $D^+\times D^-$ counterpart (3.14), we see that the difference arises in the θ-dependent function [Eqs. (4.8) here vs (3.12) before], where now $2k-1=i\kappa$ and the angle θ is a hyperbolic one. Since $\mathrm{arsinh}\,x=-i\arcsin ix$, we may use (3.18) in order to express (4.10) as hypergeometric functions of ρ_2^2/ρ^2 or ρ_1^2/ρ^2.

For the $D^1\times D^-$ coupling we have thus

$$\begin{aligned}C\begin{pmatrix}\frac14+,\frac14-;0,k\\ \rho_1\ ,\rho_2\ ;\tau,\rho\end{pmatrix}&=\delta(\rho_1^2/2-\rho_2^2/2-\tau\rho^2/2)\\ &\quad\times 2\pi^{-1/2}\rho_1^{-1/2}\rho_2^{-1/2}F\left[\begin{matrix}k-\frac12,\frac12-k\\ \frac12\end{matrix};-\frac{\rho_m^2}{\rho^2}\right],\quad k\geqslant 0,\end{aligned}\tag{4.11a}$$

$$\begin{aligned}C\begin{pmatrix}\frac34+,\frac34-;0,k\\ \rho_1\ ,\rho_2\ ;\tau,\rho\end{pmatrix}&=\delta(\rho_1^2/2-\rho_2^2/2-\tau\rho^2/2)\\ &\quad\times 2\kappa\pi^{-1/2}\rho_1^{1/2}\rho_2^{1/2}\rho^{-2}F\left[\begin{matrix}k+\frac12,\frac32-k\\ \frac32\end{matrix};-\frac{\rho_m^2}{\rho^2}\right],\quad k>0,\end{aligned}\tag{4.11b}$$

$$C\begin{pmatrix}\frac14+,\frac34-;\frac12,k\\ \rho_1\ ,\rho_2\ ;+1,\rho\end{pmatrix}=C\begin{pmatrix}\frac34+,\frac14-;\frac12,k\\ \rho_1\ ,\rho_2\ ;-1,\rho\end{pmatrix}$$

$$=C\begin{pmatrix}\frac34+,\frac34-;0,k\\ \rho_1\ ,\rho_2\ ;+1,\rho\end{pmatrix},\tag{4.11c}$$

$$C\begin{pmatrix}\frac14+,\frac34-;\frac12,k\\ \rho_1\ ,\rho_2\ ;-1,\rho\end{pmatrix}=C\begin{pmatrix}\frac34+,\frac14-;\frac12,k\\ \rho_1\ ,\rho_2\ ;-1,\rho\end{pmatrix}$$

$$=C\begin{pmatrix}\frac14+,\frac14-;0,k\\ \rho_1\ ,\rho_2\ ;+1,\rho\end{pmatrix},\tag{4.11d}$$

where

$$\rho_m=\begin{Bmatrix}\rho_2:&\rho_1>\rho_2&\text{i.e.,}&\tau=+1\\ \rho_1:&\rho_1<\rho_2,&\text{i.e.,}&\tau=-1\end{Bmatrix}=\min(\rho_1,\rho_2).\tag{4.11e}$$

4.7: Note in particular that for $k=\frac12$ ($\kappa=0$), the representation which belongs to the nonexceptional continuous series $C^0_{1/4}$ is obtained from the couplings $D^+_{1/4}\times D^-_{1/4}$. It does not appear in $D^+_{3/4}\times D^-_{3/4}$ [Eqs. (4.11a) vs (4.11b)]. For $\epsilon=\frac12$, the point $k=\frac12$ ($\kappa=0$) belongs, instead, to the $D^\pm_{1/2}$ SAIR's. That these discrete representations occur among the $D^+_\rho\times D^-_\rho$ direct integral decomposition is evident from (4.11c) and (4.11d), and in fact can be seen from (4.8c) and (4.8d): the coupling $D^+_{3/4}\times D^-_{1/4}$ contains $D^+_{1/2}$, but not $D^-_{1/2}$, while the reverse is true for $D^+_{1/4}\times D^-_{3/4}$. The fact that a discrete series representation appears (and no spurious $\epsilon=\frac12$, $k=\frac12$ C-representation) is shown by the J_- eigenvalue of the coupled state being purely positive in the first coupling, and purely negative in the second. This is the signature of a discrete—as opposed to a continuous—SAIR.

4.8: The CGC for the $D^-_\rho\times D^+_\rho$ coupling may be obtained from the $D^+_\rho\times D^-_\rho$ ones displayed above, through the application of the algebra outer automorphism A described in (2.5). The effect of $A=A_1A_2$ is to invert the sign of the spectra of the factor and coupled states under the J_- operators, so that $\tau\leftrightarrow-\tau$ through (4.11). This operator leaves $\mathscr{L}^2_{\iota_1,\iota_2}(R^2)$ invariant and is unitary under the inner product (4.3). It follows that

$$C\begin{pmatrix}k_1-,k_2+;\epsilon,k\\ \rho_1,\ \rho_2\ ;\tau,\rho\end{pmatrix}=C\begin{pmatrix}k_1+,k_2-;\epsilon,k\\ \rho_1,\ \rho_2\ ;\tau,\rho\end{pmatrix},\tag{4.12}$$

for all CGC's.

4.9: As a preparation for Secs. V–X, we shall now project the coupled operator on a definite C^ϵ_q SAIR space, using again the fact that there the coupled Q^{k_1,k_2} is a multiple of the identity. Following (3.19) and (3.20), we use a similarity transformation:

$$\begin{aligned}r^{1/2}\left(\frac{\partial^2}{\partial x_1^2}-\frac{\partial^2}{\partial x_2^2}\right)r^{-1/2}&\\ &=\sigma r^{1/2}\left(\frac{\partial^2}{\partial r^2}+r^{-1}\frac{\partial}{\partial r}+r^{-2}[4Q-1]\right)r^{-1/2}\\ &=\sigma\left(\frac{\partial^2}{\partial r^2}-\frac{\gamma}{r^2}\right),\quad \gamma=(2k-1)^2-\tfrac14=-\kappa^2-\tfrac14\leqslant-\tfrac14.\end{aligned}\tag{4.13}$$

This allows us to write the so(2,1) generators as operators on the hyperbolic coordinates $\sigma=\pm1$, $r\in R^+$ (retaining the index ϵ related to the eigenvalue ι of the inversion operator).

The expressions are

$$J_1^{\epsilon,k}=\frac{\sigma}{4}\left(-\frac{d^2}{dr^2}+\frac{\gamma}{r^2}-r^2\right),\tag{4.14a}$$

$$J_2^{\epsilon,k}=-\frac{i}{2}\left(r\frac{d}{dr}+\frac12\right),\tag{4.14b}$$

$$J_0^{\epsilon,k} = \frac{\sigma}{4}\left(-\frac{d^2}{dr^2} + \frac{\gamma}{r^2} + r^2\right), \tag{4.14c}$$

$$J_+^{\epsilon,k} = \frac{\sigma}{2}\left(-\frac{d^2}{dr^2} + \frac{\gamma}{r^2}\right), \tag{4.14d}$$

$$J_-^{\epsilon,k} = \frac{\sigma}{2} r^2. \tag{4.14e}$$

These operators are self-adjoint on the space of two-chart functions[13d,14] in $\mathscr{L}^2_{\sigma=1}(R^+)\times\mathscr{L}^2_{\sigma=-1}(R^+)$ with inner product

$$(f,g)_{\mathscr{S}} = \sum_{\sigma=\pm 1}\int_0^\infty dr\, f(\sigma,r)^* g(\sigma,r),$$
$$\mathscr{S} = \{-1,+1\}\times R^+. \tag{4.15}$$

The automorphism A exchanges charts $\sigma\leftrightarrow -\sigma$ and is unitary under (4.15).

The index ϵ, as before in (3.21), seems to be absent from the right-hand sides of (4.14). As will be seen in full detail below, it continues to exist as a specification of the domain of the operators: It indicates that we are considering the common self-adjoint extension of (4.14) in which the spectrum of $J_0^{k_1,k_2}$ is contained in $\{\epsilon + n, n\in Z\}$. In the discrete series case, for $k\geqslant 1$ there is a unique self-adjoint extension, and the index ϵ could in principle be dropped. The above operators, on the other hand, for $\gamma < \frac{3}{4}$ (including $\gamma\leqslant -\frac{1}{4}$ here) have a one-parameter family of such self-adjoint extensions.

4.10: In each chart, the operators $J_1^{\epsilon,k}$, $J_0^{\epsilon,k}$, and $J_+^{\epsilon,k}$ represent Schrödinger Hamiltonians with a strongly singular behavior at zero,[20] due to the terms γ/r^2 for $\gamma\leqslant -\frac{1}{4}$. We would like to study the features of such singular operators in $\mathscr{L}^2(R^+)$, on a single σ-chart, in particular, give a short account of the one-parameter family of self-adjoint extensions of $J_0^{\epsilon,k}$, and their spectra, both for $k\in\mathscr{D}$ and $k\in\mathscr{C}$. Then we shall do the same for the two-chart inner product (4.15), and thus make precise the applicability of (4.14) for both D^+, C as well as for the exceptional continuous representation series $E(\frac{1}{2} < k < 1)$, which does not appear in the decomposition of the product of two oscillator representations. Operators with an unbounded spectrum are not commonly used in physics, and the sharper tools of analysis must be brought to bear on the subject. From our knowledge of the so(2,1) representation series, we do expect that J_0 in our case (4.14) and (4.15) will have a spectrum given by $\epsilon + n$, $n\in Z$.

V. THE GENERALIZED OSCILLATOR ALGEBRA

The purpose of this section is to study the generalized oscillator realization of the so(2,1) algebra given by the second-order differential operators (4.14) [including (3.21) as a particular case] and to show how, through an appropriate definition of the function domains on two charts, these provide for all self-adjoint representations of the algebra.

5.1: To this end, we consider first the eigenvalue equation

$$K^k\phi_\mu^k(r) = \mu\phi_\mu^k(r), \quad r\in R^+, \tag{5.1a}$$

where K^k is J_0^k as given by (4.14) on the single chart $\sigma = 1$:

$$K^k = \frac{1}{4}\left(-\frac{d^2}{dr^2} + \frac{\gamma}{r^2} + r^2\right), \quad \gamma = (2k-1)^2 - \tfrac{1}{4}\in R, \tag{5.1b}$$

representing the Schrödinger Hamiltonian of a harmonic oscillator with a centrifugal barrier ($\gamma > 0$) or centripedal well ($\gamma < 0$). The solutions to Eq. (5.1), which vanish at infinity, are given by the Whittaker functions (Ref. 19, Eq. 13.1.33):

$$\phi_\mu^k(r) = c_\mu^k[\Gamma(k-\mu)\Gamma(1-k-\mu)]^{1/2} r^{-1/2} W_{\mu,k-1/2}(r^2)$$
$$= \phi_\mu^{1-k}(r), \tag{5.2}$$

where the Γ-function factor has been chosed for convenience. Note that the functions $\phi_\mu^k(r)$, being invariant under $k\leftrightarrow 1-k$ are real for all $k\in\mathscr{D}$, $(k>0)$ or $k\in\mathscr{C}$ $[k = (1+i\kappa)/2, \kappa\in R^+]$.

5.2: The behavior of $\phi_\mu^k(r)$ near $r = 0$ is given by

$$\phi_\mu^k(r) \underset{r\to 0^+}{\sim} c_\mu^k\{\Gamma(1-2k)[\Gamma(k-\mu)/\Gamma(1-k-\mu)]^{1/2} r^{2k-1/2}$$
$$+ \Gamma(2k-1)[\Gamma(1-k-\mu)/\Gamma(k-\mu)]^{1/2} r^{-2k+3/2}\}. \tag{5.3}$$

(i) When $k\geqslant 1$ the first summand is locally square-integrable but the second is not, unless $\mu = k+n$, $n\in Z^+$, when the Γ function in the latter's denominator makes the summand vanish. The pole in the coefficient of the first summand is an artifice of the Γ factor, and is cancelled by an appropriate normalization coefficient c_μ^k. Hence $\phi_\mu^k \in\mathscr{L}^2(R^+)$. It is, in fact, a Laguerre polynomial in r^2 of degree $\mu - k$ and order $2k-1$, times $r^{2k-1/2}\exp(-r^2/2)$. The spectrum of K^k for $k\geqslant 1$ is thus $\mu = k+n$, $\mu\in Z^+$: equally spaced and lower-bound.

(ii) When $0 < k < 1$, i.e., k is in the exceptional interval, both summands in (5.3) are locally square-integrable, and no quantization condition on μ follows from $\mathscr{L}^2(R^+)$ alone. For $\frac{1}{2} < k < 1$ the first term has a locally square-integrable derivative (and the second term must be eliminated with $\mu = k+n$, $n\in Z^+$), while when $0 < k < \frac{1}{2}$, the same is true if we exchange the first and second terms, and keep $\mu = k+n$, $n\in Z^+$. These correspond to Laguerre polynomials as above, including the case $k = \frac{1}{2}$ when proper normalization is applied.

(iii) When $k\in C$ $[k = (1+i\kappa)/2, \kappa\in R^+]$, then for all $\mu\in R$ (5.3) is in $\mathscr{L}^2(R^+)$. Its derivative does not have this property.

5.3: Although K^k formally appears to be symmetric, we find that, under the usual $\mathscr{L}^2(R^+)$ inner product (3.19),

$$(K^k\phi_\mu^k,\phi_\nu^k)_{R^+} - (\phi_\mu^k,K^k\phi_\nu^k)_{R^+} = \tfrac{1}{2}W(\phi_\mu^{k*},\phi_\nu^k)\,|_0^\infty, \tag{5.4}$$

where $W(f,g)$ is as before the Wronskian of f and g. The boundary term vanishes at infinity, while at zero it can be evaluated from (5.3). The cases for $k\in C$ and k real differ slightly but lead to the same result. The $\mathscr{L}^2(R^+)$ inner product of ϕ_μ^k and ϕ_ν^k can be thus obtained as

$$(\phi_\mu^k,\phi_\nu^k)_{R^+} = [2(\mu-\nu)]^{-1} W(\phi_\mu^{k*},\phi_\nu^k)\,|_{r\to 0}$$
$$= c_\mu^{k*} c_\nu^k \pi\csc(2\pi k)\left\{\left[\frac{\Gamma(1-k-\mu)\Gamma(k-\nu)}{\Gamma(k-\mu)\Gamma(1-k-\nu)}\right]^{1/2}\right.$$
$$\left. - \left[\frac{\Gamma(k-\mu)\Gamma(1-k-\nu)}{\Gamma(1-k-\mu)\Gamma(k-\nu)}\right]^{1/2}\right\}. \tag{5.5}$$

For each fixed $k > 0$, (5.5) vanishes when $\mu = k+m$, $m\in Z^+$, and $\nu = k+n$, $n\in Z^+$, and K^k is self-adjoint then in the Hilbert space which has $\{\phi_\mu^k\}$ as its denumerable basis.

This Hilbert space is unique when $k \geqslant 1$, but for the exceptional interval $0 < k < 1$ it is merely one of a family of Hilbert spaces: that whose denumerable basis functions have square-integrable derivatives. [This also holds for $k = \frac{1}{2}$ in spite of the apparent singularity of (5.5).] The common feature of these domains is that the spectrum of K^k is lower-bound and equally spaced, signifying that we are in the discrete series D^+_k.

5.4: In order to give a common Hilbert space domain for all generators of so(2,1) [(4.14) for fixed k and $\sigma = +1$], it is necessary to know whether a proposed domain with basis $\{\phi^k_\mu\}$ is invariant under the action of a generator basis. We are using the spectrum of $K^k = J^{k+}_0$ to specify such domains. When we construct the raising and lowering operators $J_{\uparrow\downarrow} = J_1 \pm iJ_2$ and apply them to any ϕ^k_μ, μ in the spectrum of K^k, we may employ the usual algebraic argument to show that $J_{\uparrow\downarrow}\phi^k_\mu$ should be an eigenfunction of K^k with eigenvalue $\mu \pm 1$. Unless $\mu \pm 1$ is in the spectrum of K^k when μ is, the rest of the algebra generators will not leave the domain invariant.

Lower-boundedness is no problem since it is elementary to show that $J_\downarrow \phi^k_k = 0$, but a necessary condition to be able to specify a common self-adjoint extension of all operators in so(2,1) is that the domain be such that the spectrum of K^k be equally spaced.

5.5: The domain in which K^k, for k in the exceptional interval, has a lower-bound equally spaced spectrum, however, is only a particular self-adjoint extension of the operator.[18] As said before, this is specified through the vector space on which K^k is to act. This domain can here be in turn described as those $\mathscr{L}^2(R^+)$ functions f whose boundary Wronskian $W(f,\phi_{\mu_0})\,|_0$ is to vanish, thus setting the boundary term in (5.5) to zero. This is equivalent to imposing that μ_0 be a point in the spectrum of the operator.

It can be shown that, for k in $(\frac{1}{2},1)$, the spectrum of each self-adjoint extension of K^k has a lower bound, but this minimum eigenvalue has itself no lower bound, so that extensions can be found where this minimum is as negative large as we please. For $k \in C$ the spectrum has no lower bound. Two more general results[18] are that the union of all self-adjoint extensions provide spectra which cover the real line. No eigenvalue μ_0 can belong to the spectrum of more than one self-adjoint extension of K^k.

Given thus some μ_0, finding the rest of the spectrum is an exercise in solving for ν the transcendental equation

$$\Gamma(k-\nu)/\Gamma(1-k-\nu) = \Gamma(k-\mu_0)/\Gamma(1-k-\mu_0), \tag{5.6}$$

which puts to zero the last expression in (5.5). As a numerical example, if for $k = \frac{5}{6}$ we choose $\mu_0 = -1$, the spectrum of K^k will be (up to three decimal places) $\{-1.0, 1.046, 2.097, 3.123, 4.141, 5.153, 6.163, 7.170, 8.176, 8.179, 9.182, \cdots\}$, while if for $k = \frac{1}{2} + i$ we choose $\mu_0 = 0$, the spectrum will be $\{\cdots, -8.881, 0.0, 1.449, 2.619, 3.727, 4.806, 5.869, 6.921, 7.965, \cdots\}$. These eigenvalues tend asymptotically toward equal spacing; but the spectrum is not linear, and the domain specified by $\mu_0 \in R$, for $\mu_0 - k$ not a positive integer, is therefore not fit to serve as a common invariant domain for a set of operators which are to be elements of a Lie algebra.

5.6: We shall now see what the choice of self-adjoint extensions is for the two-chart operator $J^{\epsilon,k}_0$ in (4.14c) with inner product (4.15). The eigenvalue equation to be solved now has two forms, one in each chart $\sigma = \pm 1$. Since $J^{\epsilon,k}_0 = \sigma K^k$, the equations are

$$K^k\psi^k_\mu(\sigma = +1, r) = \mu\psi^k_\mu(\sigma = +1, r), \tag{5.7a}$$

$$-K^k\psi^k_\mu(\sigma = -1, r) = \mu\psi^k_\mu(\sigma = -1, r). \tag{5.7b}$$

The difference with (5.1) appears to be slight. We can set

$$\psi^k_\mu(\sigma = +1, r) = \phi^k_\mu(r), \quad \psi^k_\mu(\sigma = -1, r) = a^k_\mu \phi^k_{-\mu}(r), \tag{5.7c}$$

with a^k_μ a constant to be determined. We now repeat (5.4) under the inner product (4.15):

$$(J^k_0\psi^k_\mu, \psi^k_\nu)_{\mathscr{S}} - (\psi^k_\mu, J^k_0\psi^k_\nu)_{\mathscr{S}} = \tfrac{1}{2}W(\phi^{k*}_\mu, \phi^k_\nu)\,|_{r=0} - \tfrac{1}{2}a^{k*}_\mu a^k_\nu W(\phi^{k*}_{-\mu}, \phi^k_{-\mu})\,|_{r=0}. \tag{5.8}$$

Upon performing the necessary algebra with (5.5), we can see that whenever $\mu - \nu$ is an integer, a full cancellation of the boundary terms occurs for $a^k_\mu = 1 = a^k_\nu$. The normalization constant c^k_μ of the constituent functions (5.2) may be found along the lines of subsection 3.5, or directly through integral tables (Ref. 2, Eqs. 7.6114 and 8.365.9). If we denote $\mu = \epsilon + n$, $\epsilon \in (-\frac{1}{2}, \frac{1}{2}]$, $n \in Z$, c^k_μ depends only on k and ϵ [this feature determined the Γ-function choice in (5.2)]. It is

$$c^k_\mu = c^{\epsilon k} = \pi^{-1}[2\sin\pi(k-\epsilon)\sin\pi(k+\epsilon)]^{1/2} = c^{\epsilon,1-k} = c^{-\epsilon,k}. \tag{5.9}$$

If $k \in C$, the functions $\psi^{\epsilon k}_\mu(\sigma, r)$ are the eigenfunctions of the self-adjoint extension of the operator $J^{\epsilon k}_0$ with spectrum $\mu \in \{\epsilon + n, n \in Z\}$. This extension may be labeled through the index $\epsilon \in (-\frac{1}{2}, \frac{1}{2}]$, which generalizes the previously used homonym index $\epsilon \in (0, \frac{1}{2})$ to multivalued representations of the group.

When $\epsilon = \frac{1}{2}$, the limit $k = (1 + i\kappa)/2$, $\kappa \to 0$, results in $c^{\epsilon k}$ becoming zero. For $\psi^k_\mu(+1, r)$, $\mu = \frac{1}{2}, \frac{3}{2}, \cdots$, this zero is compensated, however, by a matching pole from the Γ functions in (5.2); similarly, only the $\sigma = -1$ component of $\psi^k_\mu(\sigma, r)$, $\mu = -\frac{1}{2}, -\frac{3}{2}, \cdots$, is nonzero. These functions therefore belong to the discrete series of SAIR's, having a single-chart support.

5.7: The algebra generators (4.14) belong to the exceptional continuous SAIR series E when $0 < k < 1$ ($-\frac{1}{4} \leqslant \gamma < \frac{3}{4}$ twice). The domain is that labeled by ϵ, with $|\epsilon| < \min(k, 1-k)$ so that the radicand in (5.9) is positive. Since reflection symmetry $k \leftrightarrow 1-k$ holds, we may reduce to $\frac{1}{2} < k < 1$ and $|\epsilon| < 1 - k$. The spectrum of $J^{\epsilon,k}_0$ is in this case again given by $\mu \in \{\epsilon + n, n \in Z\}$.

We shall now examine the boundary of the exceptional series region (Fig. 1), $|\epsilon| = \min(k, 1-k)$, which gives rise to the lower- and upper-bound discrete series $D^\pm_k$ in the interval $0 < k < 1$, including the two direct summands of the oscillator representation. There is an interplay between the zeros of $c^{\epsilon k}$ in (5.9) and the Φ-function poles in the factor of (5.2). Consider the $\sigma = +1$ component and see Fig. 1. When $0 < \epsilon = k \leqslant \frac{1}{2}$ or $0 > \epsilon = k - 1 \geqslant -\frac{1}{2}$, the only nonzero func-

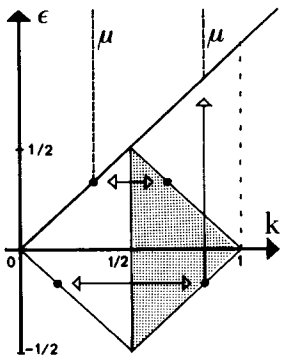

FIG. 1. The exceptional interval. The shaded region indicates the range of k and ϵ for the continuous exceptional series, $|\epsilon| < 1 - k$, where the $k \leftrightarrow 1 - k$ symmetry is used to reduce k to $(\frac{1}{2},1)$. The boundary corresponds to the discrete series. The points $0 < \epsilon = k$ (for $0 < k \leqslant \frac{1}{2}$) and $0 < \epsilon = 1 - k$ (for $\frac{1}{2} \leqslant k < 1$) lead to eigenfunctions ψ^k_μ with spectrum $\{\epsilon + n, n \in Z^+\}$, while $0 > \epsilon = k - 1$ (for $\frac{1}{2} \geqslant k > 1$) and $0 > \epsilon = -k$ (for $0 < k \leqslant \frac{1}{2}$) lead to $\{\epsilon + n + 1, n \in Z^+\}$.

tions with $\mu = \epsilon + n$, $n \in Z$, are those with $\mu = k, k+1, k+2, \cdots$ while when $0 > \epsilon = -k \geqslant -\frac{1}{2}$ or $0 < \epsilon = 1 - k \leqslant \frac{1}{2}$, the only nonzero functions with $\mu = \epsilon + n$, $n \in Z$, are those with $\mu = 1 - k, 2 - k, 3 - k, \cdots$. As an example, $\epsilon = \frac{1}{4}$, $k = \frac{1}{4}$, and $\epsilon = \frac{1}{4}$, $k = \frac{3}{4}$ characterize the same self-adjoint extension in the even positive harmonic oscillator state space, while $\epsilon = -\frac{1}{4}$, $k = \frac{1}{4}$ and $\epsilon = \frac{1}{4}$, $k = \frac{3}{4}$ characterize the odd oscillator state space. The operator K^k, is, of course, the same under the exchange $k \leftrightarrow 1 - k$. The above arguments, however, lead us to drop this symmetry and adopt $k \in (0,1)$ as the sole indicator of the self-adjoint extension of the algebra meant for the discrete series in the exceptional interval, as was done in point (ii) early in this section.

The same reasoning holds for the $\sigma = -1$ chart of the wavefunctions $\psi^k_\mu(\sigma,r)$, under the exchange $\mu \leftrightarrow -\mu$, leading to basis functions for the upper-bound negative discrete series D^-_k. For $k \geqslant 1$ we are left, thus, with a description of the discrete series in terms of a direct sum of two function spaces, where $\psi^k_\mu(\sigma,r)$ with $\mu = k, k+1, \cdots$ has only a $\sigma = +1$ chart support, and with $\mu = -k, -k-1, \cdots$ has only a $\sigma = -1$ chart support. These constitute single-chart SAIR bases for D^+_k and D^-_k, respectively.

The outer automorphism A effecting (2.5a) may be properly defined on functions of $\mathscr{S}$ through

$$Af(\sigma,r) = f(-\sigma,r). \tag{5.10}$$

It exchanges the lower- and upper-bound discrete SAIR spaces and leaves invariant the continuous series SAIR spaces.

5.8: As a conclusion to the last four sections, we should like to restate that the so(2,1) algebra realized through the set of formal second-order differential operators given in (4.14) for any real γ, on spaces of functions on $\mathscr{S} = \{-1, +1\} \times R^+$ with self-adjoint extensions in $\mathscr{L}^2(\mathscr{S})$ specified through the index ϵ in the manner brought out above, accommodates all the SAIR's of the algebra. We have devoted some space to show that this is true for the continuous $\mathscr{C}$ series, and justified that the more naive treatments found in the literature for the $\mathscr{D}$ case are also appropriate. In the next section we proceed to generalize the construction of the CGC's for general SAIR products.

VI. THE COUPLING OF TWO GENERAL REPRESENTATIONS

The tactics seen in Secs. III and IV provide us now with the strategy for coupling any pair of so(2,1) SAIR's as described in Sec. V.

6.1: We shall have two sets of operators (4.14) in two independent sets of variables $\sigma_1, r_1 \in \mathscr{S}$ and $\sigma_2, r_2 \in \mathscr{S}$ generating $\mathscr{D}$ and/or $\mathscr{C}$ representations. The factor operator sets $J^{k_j}_{(j)\alpha}$, $j = 1,2$, will refer to these variables, while the coupled operators will be, as before,

$$J_\alpha = J^{k_1}_{(1)\alpha} + J^{k_2}_{(2)\alpha}, \quad \alpha = 1,2,0,+,-. \tag{6.1}$$

The labels k_j are assumed to contain all the SAIR information, appearing as $k_j \pm$ for $\mathscr{D}$ and ϵ_j, k_j for $\mathscr{C}$. The domain of the operators will be the set of two-variable functions which belong, as functions of each, to the Hilbert spaces specified in the last section, where the spectrum of $J^{k_j}_{(j)0}$ is contained in $\{\epsilon_j + n, n \in Z\}$ understanding that for D^+, $\epsilon_j \equiv k_j$, modulo unity. The defining inner product may be written as

$$(\phi,\chi)_{\mathscr{S}^2} = \sum_{\sigma_1,\sigma_2 = \pm 1} \int_0^\infty dr_1 \int_0^\infty dr_2\, \phi(\sigma_1,r_1,\sigma_2,r_2)^* \times \chi(\sigma_1,r_1,\sigma_2,r_2). \tag{6.2}$$

We recall, finally that when one or both of the factor SAIR's belong to $D^\pm$, the support of the functions will be the $\sigma_j = \pm 1$ chart only.

6.2: The product states

$$\psi^{k_1,k_2}_{\tau_1,\rho_1,\tau_2,\rho_2}(\sigma_1,r_1,\sigma_2,r_2) = \delta_{\sigma_1,\tau_1}\delta_{\sigma_2,\tau_2}(\rho_1\rho_2)^{-1/2} \times \delta(r_1 - \rho_1)\delta(r_2 - \rho_2) \tag{6.3}$$

are the generalized eigenfunctions of the following set of commuting operators:

(i) $Q^{k_1}_{(1)}$ and $Q^{k_2}_{(2)}$ (realized as multiples of the identity) with eigenvalues $q_1 = k_1(1 - k_1)$, $q_2 = k_2(1 - k_2)$.

(ii) $J^{k_1}_{(1)-}$ and $J^{k_2}_{(2)-}$ with eigenvalues $\tau_1\rho_1^2/2$ and $\tau_2\rho_2^2/2$, respectively $(\tau_j \in \{-1,1\}, \rho_j \in R^+, j = 1,2)$. For $D^+_{k_j}$, τ_j is identically $+1$, and for $D^-_{k_j}$, $\tau_j = -1$.

(iii) The common domain of the above two-variable operators is taken to be the space described in the last section, specified by ϵ_1, ϵ_2. A denumerable basis for this space is $\psi^{k_1}_{\mu_1}(\sigma_1,r_1)\psi^{k_2}_{\mu_2}(\sigma_2,r_2)$ with $\pm\mu_j \in \{k_j + n, n \in Z^+\}$ for $D^\pm \ni k_j \equiv \epsilon_j \pmod 1$ and $\mu_j \in \{\epsilon_j + n, n \in Z\}$ for $k_j \in \mathscr{C}$. In the special case when ϵ_1, ϵ_2 are in $\{0, \frac{1}{2}\}$ the product states can be alternatively placed in the domain where the inversion operators $I_{(1)}$ and $I_{(2)}$ have eigenvalues ι_1 and ι_2 in $\{-1, +1\}$. The product states (6.3) are Dirac-orthonormal under (5.2):

$$(\psi^{k_1,k_2}_{\tau_1,\rho_1,\tau_2,\rho_2}, \psi^{k_1,k_2}_{\tau_1',\rho_1',\tau_2',\rho_2'})_{\mathscr{S}^2} = \delta(\tau_1\rho_1^2/2 - \tau_1'\rho_1'^2/2) \times \delta(\tau_2\rho_2^2/2 - \tau_2'\rho_2'^2/2). \tag{6.4}$$

6.3: The coupled states, denoted by $\Psi^{k_1,k_2}_{k,\tau,\rho}$, are the generalized eigenfunctions of the commuting operators:

(i') $Q^{k_1}_{(1)}$ and $Q^{k_2}_{(2)}$ with eigenvalues $q_1 = k_1(1 - k_1)$, $q_2 = k_2(1 - k_2)$ as before.

(ii') of the parabolic subalgebra generator

$$J_- = J^{k_1}_{(1)-} + J^{k_2}_{(2)-} = \sigma_1 r_1^2/2 + \sigma_2 r_2^2/2 = \sigma r^2/2 \quad (6.5)$$

[where in the last expression $\sigma \in \{-1,1\}$ and $r \in R^+$ will be properly defined below] with eigenvalue $\tau\rho^2/2$ ($\tau \in \{-1,1\}$ $\rho \in R^+$). Again, if the coupled SAIR belongs to $D^\pm$, the eigenvalue will be in $R^\pm$, so only $\tau = +1$ or $\tau = -1$ is allowed, while if it belongs to $\mathscr{C}$ it will be in R. Generalized eigenfunctions of (6.5) will thus have a factor $\delta(\sigma r^2/2 - \tau\rho^2/2) = \delta_{\sigma,\tau}\delta(r^2/2 - \rho^2/2)$ as in (4.6).

(iii′) The spectrum of the compact generator $J_0 = J^{k_1}_{(1)0} + J^{k_2}_{(2)0}$ as seen in Sec. V defines the self-adjoint extension domain. Here it is $\mu = \mu_1 + \mu_2$. Modulo integers, this implies that the coupled SAIR space is characterized by

$$\epsilon \equiv \epsilon_1 + \epsilon_2 \pmod 1. \quad (6.6)$$

Again, in the case when $\epsilon_1, \epsilon_2 \in \{0, \frac{1}{2}\}$ we may make use of the inversion operator $I = I_{(1)}I_{(2)}$ with eigenvalue $\iota = \iota_1\iota_2$, implying (6.6). This restricts the coupled SAIR's in a form analogous to the familiar rotation group coupling between vector and spinor UIR's.

(iv′) of the coupled Casimir operator Q, built as in (2.2) out of the coupled generators J_α, with eigenvalue $q = k(1-k)$. The explicit form of Q in terms of the $\mathscr{S}^2$ space variables $(\sigma_1,r_1,\sigma_2,r_2)$ is

$$\begin{aligned} Q &= (J_1)^2 + (J_2)^2 - (J_0)^2 = Q^{k_1}_{(1)} + Q^{k_2}_{(2)} \\ &\quad + 2\left[J^{k_1}_{(1)1}J^{k_2}_{(2)1} + J^{k_1}_{(1)2}J^{k_2}_{(2)2} - J^{k_1}_{(1)0}J^{k_2}_{(2)0}\right] \\ &= \frac{1}{4}\left[\sigma_1\sigma_2\left(r_1\frac{\partial}{\partial r_2} - \sigma_1\sigma_2 r_2\frac{\partial}{\partial r_1}\right)^2 \right. \\ &\quad \left. - \gamma_1\left(1 + \frac{\sigma_1\sigma_2 r_1^2}{r_1^2}\right) - \gamma_2\left(1 + \frac{\sigma_1\sigma_2 r_1^2}{r_2^2}\right) + 1\right]. \end{aligned} \quad (6.7)$$

6.4: We shall now parametrize the space $\mathscr{S}^2$ in a manner which encompasses the polar and hyperbolic coordinates used in Sec. III and IV. Only the case $\sigma_1 = \sigma_2$ appeared in Sec. III, and only $\sigma_1 = -\sigma_2$ in Sec. IV. On account of the two dichotomic indices σ_1,σ_2, we have four coordinate charts. In attention to the defintion in the last equality in (6.5), in accordance with $r_1 \gtrless r_2$, two of these charts will be reparametrized, so that we have a total of six charts as follows:

(i) $P^\pm$-charts:

$$\begin{aligned} &\text{for } \sigma_1 = \pm 1 = \sigma_2, \quad r_1, r_2 \in R^+; \quad \sigma = \pm 1, \text{ respectively,} \\ &r_1 = r\cos\theta, \quad r_2 = r\sin\theta, \qquad r \in R^+, \quad \theta \in [0, \pi/2]. \end{aligned} \quad (6.8a)$$

(ii) $H^\pm_>$-charts:

$$\begin{aligned} &\text{for } \sigma_1 = \pm 1 = -\sigma_2, \quad r_1 > r_2; \quad \sigma = \pm 1, \text{ respectively,} \\ &r_1 = r\cosh\theta, \quad r_2 = r\sinh\theta, \qquad r \in R^+, \quad \theta \in [0, \infty). \end{aligned} \quad (6.8b)$$

(iii) $H^\pm_<$-charts:

$$\begin{aligned} &\text{for } \sigma_1 = \mp 1 = -\sigma_2, \quad r_1 < r_2; \quad \sigma = \pm 1, \text{ respectively,} \\ &r_1 = r\sinh\theta, \quad r_2 = r\cosh\theta, \qquad r \in R^+, \quad \theta \in [0, \infty). \end{aligned} \quad (6.8c)$$

To this list we should add two more charts for the line manifolds $\sigma_1 = -\sigma_2, r_1 = r_2$ but, since these are of lower dimension we may disregard them in what follows.

A single function $\phi(\sigma_1,r_1,\sigma_2,r_2)$ over $\mathscr{S}^2$, when the coordinates of $\mathscr{S}^2$ are expressed in terms of (r,θ) in chart C, will be represented by a function $\phi^C(r,\theta)$. The set of six such functions $\{\phi^C, C = P^\sigma, H^\sigma_>, H^\sigma_<, \sigma = \pm 1\}$ constitutes the original ϕ in the new coordinate system (C,r,θ).

We have found it useful to depict the six charts as in Fig. 2, considering the product $\sigma_j r_j$ as if it were a coordinate for R. The $D^+ \times D^+$ coupling (Sec. VII) will require only one chart: the first quadrant P^+, since $\sigma_1 = +1 = \sigma_2$, in complete analogy with Sec. III, had we halved r to R^+ through parity. The $D^+ \times D^-$ coupling (Sec. VIII), having $\sigma_1 = +1 = -\sigma_2$, will require the two charts, $H^+_>$ and $H^-_<$, in the fourth quadrant. In Sec. IX we treat the $D^+ \times \mathscr{C}$ coupling, where $\sigma_1 = +1, \sigma_2 = \pm 1$, so that the right half-plane of Fig. 2 is needed and will be covered by the three-coordinate charts P^+, $H^+_>$, and $H^-_<$. Finally, the $\mathscr{C} \times \mathscr{C}$ coupling in Sec. X requires all six charts. The joint consideration of the required number of charts is important since the product and coupled operators will continue to be self-adjoint in the corresponding space (6.6) only if the formal replacement of variables $(\sigma_1,r_1,\sigma_2,r_2) \to (C,r,\theta)$ through (6.8) is made on the appropriate union of charts. The form of J_- in (6.5) has been tailored to that purpose.

6.5: The Casimir operator (6.7) has the three following forms in each of the charts (6.8):

(i) in $P^\pm$:

$$Q = \frac{1}{4}\left[\frac{d^2}{d\theta^2} - \gamma_1\sec^2\theta + \gamma_2\csc^2\theta + 1\right], \quad (6.9a)$$

(ii) in $H^\pm_>$:

$$Q = \frac{1}{4}\left[-\frac{d^2}{d\theta^2} - \gamma_1\operatorname{sech}^2\theta + \gamma_2\operatorname{csch}^2\theta + 1\right], \quad (6.9b)$$

(iii) in $H^\pm_<$:

$$Q = \frac{1}{4}\left[-\frac{d^2}{d\theta^2} + \gamma_1\operatorname{csch}^2\theta - \gamma_2\operatorname{sech}^2\theta + 1\right], \quad (6.9c)$$

generalizing thus (3.9) and(4.5).

6.6: The inner product (6.2) defining the Hilbert space will be expressible as

$$\begin{aligned} (\phi,\chi)_{\mathscr{S}^2} = \sum_{\sigma=\pm 1} &\left[(\phi^{P^\sigma},\chi^{P^\sigma})_P + (\phi^{H^\sigma_>},\chi^{H^\sigma_>})_H \right. \\ &\left. + (\phi^{H^\sigma_<},\chi^{H^\sigma_<})_H\right], \end{aligned} \quad (6.10a)$$

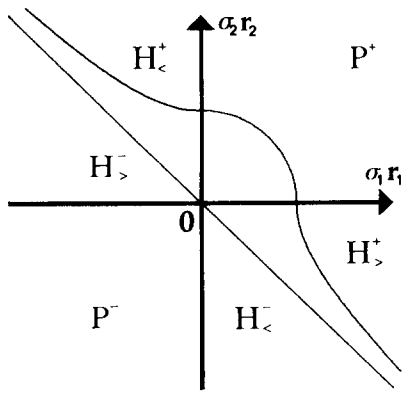

FIG. 2. The six coordinate charts in $\mathscr{S}^2$.

$$(\alpha,\beta)_P = \int_0^\infty r\,dr \int_0^{\pi/2} d\theta\, \alpha(r,\theta)^*\beta(r,\theta), \tag{6.10b}$$

$$(\alpha,\beta)_H = \int_0^\infty r\,dr \int_0^\infty d\theta\, \alpha(r,\theta)^*\beta(r,\theta). \tag{6.10c}$$

Although each of the formal operators (6.9) may be separately self-adjoint under (6.10b) or under one of (6.10c) in some appropriate one-chart Hilbert space, Q itself, as represented by all three forms (6.9), will have the proper spectrum only when placed in the full inner product (6.10), and only there will the orthogonality of the expected eigenfunctions hold consistent with (6.6). When a subspace of functions is identically zero in some charts (as in the $D^+ \times D^+$ case where the support lies entirely in the P^+ chart), the inner product may be reduced to a subset of the summands [to (6.10b) alone, with $\sigma = +1$ in the $D^+ \times D^+$ case].

6.7: Since the coupled states are eigenstates of J_- with eigenvalue $\tau\rho^2/2$, they will contain, as discussed above, a factor of $\delta_{\sigma\tau}\,\delta(r^2/2 - \rho^2/2)$. The Kronecker δ restricts the support of the function to the upper ($\sigma = \tau = +1$) or lower ($\sigma = \tau = -1$) diagonal half-planes in Fig. 2; the Dirac δ restricts the support further to a constant value of r^2; as shown in the figure, this is a quarter-circle in the P^σ-chart, and a quarter-hyperbola in the $H^\sigma_>$ and $H^\sigma_<$ charts.

As before [cf. Eqs. (3.10) and (4.6)], we write the product state as

$$\Psi^{k_1,k_2,C^\sigma}_{k,\tau,\rho}(r,\theta) = \delta_{\sigma,\tau}\delta(r^2/2 - \rho^2/2)F^C_{k,\tau}(\theta), \tag{6.11}$$

the index C^σ standing for a specification of the chart. The requirement that they be eigenfunctions of the Casimir operator (6.9) with eigenvalue $k(1-k)$ leads to the following differential equations for the θ-dependent factor:

(i) on the P-charts, $\theta\in[0,\pi/2]$:

$$\left[-\frac{d^2}{d\theta^2} + \gamma_1\sec^2\theta + \gamma_2\csc^2\theta\right]F^P_{k,\tau}(\theta) = (2k-1)^2F^P_{k,\tau}(\theta); \tag{6.12a}$$

(ii) on the $H_>$-charts, $\theta\in[0,\infty)$:

$$\left[-\frac{d^2}{d\theta^2} - \gamma_1\operatorname{sech}^2\theta + \gamma_2\operatorname{csch}^2\theta\right]F^{H_>}_{k,\tau}(\theta) = -(2k-1)^2F^{H_>}_{k,\tau}(\theta); \tag{6.12b}$$

(iii) on the $H_<$-charts, $\theta\in[0,\infty)$:

$$\left[-\frac{d^2}{d\theta^2} + \gamma_1\operatorname{csch}^2\theta - \gamma_2\operatorname{sech}^2\theta\right]F^{H_<}_{k,\tau}(\theta) = -(2k-1)^2F^{H_<}_{k,\tau}(\theta). \tag{6.12c}$$

We recall that $\gamma_j = (2k_j - 1)^2 - \frac{1}{4}$ for all cases, so that $\gamma_j > -\frac{1}{4}$ for $k_j\in\mathscr{D}$, and $\gamma_j < (1-2|\epsilon_j|)^2 - \frac{1}{4}$ for $k_j\in\mathscr{C}$, and the exceptional interval $0<k<1$ corresponds to $-\frac{1}{4}\leqslant\gamma_j<\frac{3}{4}$. Equation (6.12a) is the Schrödinger equation for a Pöschl–Teller potential[16] of the first kind, while Eqs. (6.12b) and (6.12c) (which only exchange $\gamma_1\leftrightarrow\gamma_2$) are Schrödinger equations for Pöschl–Teller potentials of the second kind. The singularities of the potentials [$\theta = 0$ and $\pi/2$ in (6.12a), and $\theta = 0$ in (6.12b) and (6.12c)] are of the inverse-quadratic type, and in Fig. 2 can be seen to lie on the coordinate axes: The value of k_1 provides the coefficient γ_1 of the singularity on the $r_1 = 0$ axis ($\theta = \pi/2$ in P, $\theta = 0$ in $H_<$), and k_2 the coefficient γ_2 of that on the $r_2 = 0$ axis ($\theta = 0$ in P, $\theta = 0$ in $H_>$).

In the two H cases, the potential tends exponentially to zero at $\theta\to\infty$. As we shall see in detail in the following four sections, when the support of the functions $F_{k,\tau}(\theta)$ is further restricted by a discrete-series factor SAIR $D^\pm$ through the values of σ_1, σ_2 to a quadrant or half-plane in Fig. 2, the region is delimited: A strong barrier[21] (i.e., an inverse-quadratic singularity with coefficient $\gamma_j\geqslant\frac{3}{4}$) or a weak barrier/well (of coefficient $-\frac{1}{4}\leqslant\gamma_j\leqslant\frac{3}{4}$) appears at the edge, according to whether $k\geqslant 1$ or $0<k<1$. For continuous series factor SAIR's, when two charts must be "joined" through the cancellation of the boundary Wronskians, the potential singularity which lies at the "common boundary" is a strong well[21] (i.e., of coefficient $\gamma_j\leqslant -\frac{1}{4}$) or a weak barrier/well according to whether $k_j\in C$ or $k_j\in E$.

A strong barrier at θ_0 imposes a choice of one of the two solutions of (6.12) through requiring that it be locally $\mathscr{L}^2$. A weak barrier/well singularity exhibits two locally $\mathscr{L}^2$-solutions, and allows for a choice: The solutions with locally $\mathscr{L}^2$-derivatives are to be taken for $\mathscr{D}$. A strong well at θ_0 also has two solutions, but no naturally distinguished ones. The proper cancellation of the boundary Wronskians will determine—up to constants in some cases—the total multichart solutions where the Casimir operator is to be self-adjoint and which must match (6.6). We shall defer further discussion on this aspect to Secs. IX and X, where this is done in detail for the cases at hand.

Lastly, the sign of the "energy" eigenvalue $(2k-1)^2$ should be noticed on the right-hand side of Eqs. (6.12). For continuous-series coupled SAIR's, $F^{H_>}$ and $F^{H_<}$ are "positive-energy" free states, while for $k\in\mathscr{D}$ they appear as "negative-energy" bound states in the well of the Pöschl–Teller potential. For the P^σ-chart, (6.12a), the roles are reversed and the discrete-series coupled SAIR's appear as positive-energy quantized states between potential barriers in the $D^+ \times D^+$ coupling. In the $D^+ \times \mathscr{C}$ and $\mathscr{C}\times\mathscr{C}$ couplings, the P^σ-chart must be matched with one or two H-charts, so it should not come as a surprise that in the P-chart the continuum C states appear under the D states. The $k = \frac{1}{2}$ level corresponds to zero "energy," and may in principle belong to $D^\pm_{1/2}$ or $C^\epsilon_{1/4}$ ($\epsilon\neq\frac{1}{2}$). Couplings to the exceptional continuous SAIR E can only appear as levels between values 0 and -1 of the H-chart "energy" $-(2k-1)^2$; they may be recognized through seeing that $|\epsilon| < \min(k, 1-k)$.

6.8: The general solution for the Pöschl–Teller Schrödinger equations (6.12) can be written as a linear combination of two of the fundamental solutions of the hypergeometric equation. In order to use uniformly the nomenclature of Ref. 19, p. 563, we may define, in each chart, the variable Θ as:

(i) P-charts, $\theta\in[0,\pi/2]$:

$$\Theta = \theta, \quad \sin\Theta = \sin\theta = r_2/r, \quad \cos\Theta = \cos\theta = r_1/r; \tag{6.13a}$$

(ii) $H_>$-charts, $\theta\in[0,\infty)$:

$$\Theta = i\theta, \quad \sin\Theta = i\sinh\theta = ir_2/r,$$

$$\cos\Theta = \cosh\theta = r_1/r; \tag{6.13b}$$

(iii) $H_<$-charts, $\theta\in[0,\infty)$:

$$\Theta = i\theta + \pi/2, \quad \sin\Theta = \cosh\theta = r_2/r,$$

$$\cos\Theta = -i\sinh\theta = -ir_1/r. \tag{6.13c}$$

The solutions of (6.12) can now be written in terms of the Gauss hypergeometric series expansions around $\Theta = 0, \pi/2, \infty$:

$$w^{k_1,k_2,k}_{1(0)}(\Theta) = w^{1-k_1,k_2,k}_{1(0)}(\Theta) = w^{k_1,k_2,1-k}_{1(0)}(\Theta)$$
$$= |\cos\Theta|^{2k_1-1/2}|\sin\Theta|^{2k_2-1/2}$$
$$\times F\left[\begin{matrix}k_1+k_2-k, k_1+k_2+k-1\\ 2k_2\end{matrix};\sin^2\Theta\right], \tag{6.14a}$$

$$w^{k_1,k_2,k}_{2(0)}(\Theta) = w^{k_1,1-k_2,k}_{1(0)}(\Theta), \tag{6.14b}$$

$$w^{k_1,k_2,k}_{1(1)}(\Theta) = w^{k_1,1-k_2,k}_{1(1)}(\Theta) = w^{k_1,k_2,1-k}_{1(1)}(\Theta)$$
$$= w^{k_2,k_1,k}_{1(0)}(\Theta \pm \pi/2)$$
$$= |\cos\Theta|^{2k_1-1/2}|\sin\Theta|^{2k_2-1/2}$$
$$\times F\left[\begin{matrix}k_1+k_2-k, k_1+k_2+k-1\\ 2k_1\end{matrix};\cos^2\Theta\right], \tag{6.15a}$$

$$w^{k_1,k_2,k}_{2(1)}(\Theta) = w^{1-k_1,k_2,k}_{1(1)}(\Theta), \tag{6.15b}$$

$$w^{k_1,k_2,k}_{1(\infty)}(\Theta) = w^{k_1,1-k_2,k}_{1(\infty)}(\Theta) = S_C^{2k_1-1} w^{1-k_1,k_2,k}_{1(\infty)}(\Theta)$$
$$= S_C^{-k_1-k_2+k} w^{k_2,k_1,k}_{1(\infty)}(\Theta \pm \pi/2)$$
$$= |\cos\Theta|^{2k_1-1/2}|\sin\Theta|^{-2k_1+2k-1/2}$$
$$\times F\left[\begin{matrix}k_1+k_2-k, k_1-k_2-k+1\\ 2-2k\end{matrix};\csc^2\Theta\right], \tag{6.16a}$$

$$w^{k_1,k_2,k}_{2(\infty)}(\Theta) = w^{1-k_1,1-k_2,1-k}_{1(\infty)}(\Theta) = S_C^{2k_1-1} w^{k_1,k_2,1-k}_{1(\infty)}(\Theta). \tag{6.16b}$$

In the last two equations, $S_C = +1$ for $C = H_>, H_<$, while $S_C = -1$ for $C = P$; the multivaluation is due to the Gauss function being evaluated on the branch cut (these cases will not be used, however). An identity due to a Kummer transformation (Ref. 19, Eq. 15.3.4) is

$$w^{k_1,k_2,k}_{n(\infty)}(\theta_{H_<}) = w^{k_2,k_1,k}_{n(\infty)}(\theta_{H_>}), \quad n = 1,2, \tag{6.16c}$$

between the hyperbolic cases, which exchanges $\cosh\theta \leftrightarrow \sinh\theta$ in the first two factors, and $1/\cosh^2\theta \leftrightarrow -1/\sinh^2\theta$ in the Gauss function argument. The absolute value of $\cos\Theta$ and $\sin\Theta$ has been placed on the first two factors of (6.14)–(6.16) in order to have real solutions for the $\mathscr{C}$-cases. If $2k_1$, $2k_2$, and/or $2k$ are integers, one of each pair of solutions is degenerate, and the logarithmic solution should replace it (these cases will also never be used).

In the P-charts ($\Theta\in[0,\pi/2]$) the argument of the hypergeometric functions in (5.16) ranges, for $w_{n(0)}$, $n = 1,2$, over $[0,1]$, and for $w_{n(1)}$, over $[1,0]$; for $w_{n(\infty)}$ however, the range is $(\infty,1]$, which lies on the branch cut of the Gauss function. The latter pair of solutions, therefore, will be avoided in describing solutions in the P^σ-chart. Similarly, and for the same reason, in the $H_>$-charts ($\Theta\in[0,i\infty)$) we shall avoid the $w_{n(1)}$ functions, and in the $H_<$-charts ($\Theta\in[\pi/2, \pi/2+i\infty)$) we avoid the $w_{n(1)}$ functions.

Elementary properties of these solutions which will be used time and again are their behavior near the expansion centers: $w^{k_1,k_2,k}_{1(0)}(\Theta) \sim \Theta^{2k_2-1/2}$ for $\Theta\to 0^+$, $w^{k_1,k_2,k}_{1(1)}(\Theta) \sim (\pi/2-\Theta)^{2k_1-1/2}$ for $\Theta\to\pi/2^-$, and $w^{k_1,k_2,k}_{1(\infty)}(\Theta) \sim (e^\Theta/2)^{2k-1/2}$ for $\Theta = i\theta$ or $i\theta+\pi/2$ when $\theta\to\infty$. The behavior of $w^{k_1,k_2,k}_{2(N)}(\Theta)$ can be obtained through exchanging $k_2\leftrightarrow 1-k_2$, $k_1\leftrightarrow 1-k_1$, and $k\leftrightarrow 1-k$, respectively.

6.9: In the following sections we shall use the above solutions to build the properly normalized product state through the condition that they be (Dirac-) orthonormal under the inner product (6.10a):

$$(\Psi^{k_1,k_2}_{k,\tau,\rho}, \Psi^{k_1,k_2}_{k',\tau',\rho'})_{\mathscr{S}^2} = \delta_{\tau,\tau'}\delta(\rho^2/2 - \rho'^2/2)\delta[k,k'], \tag{6.17a}$$

$$\delta[k,k'] = \begin{cases}\delta_{k,k'}, & k,k'\in D,\\ \delta(\kappa-\kappa'), & k = (1+i\kappa)/2\in C \text{ or } k = (1+\kappa)/2\in E,\\ 0, & \text{otherwise.}\end{cases} \tag{6.17b}$$

The factorization (6.11) placed in (6.10) and the above requirement lead to the (Dirac-) orthonormality condition

$$(F_{k,\tau}, F_{k',\tau'})_{s^2} = \delta_{\tau,\tau'}\delta[k,k'], \tag{6.17c}$$

where we define the reduced inner product over θ to be

$$(f,g)_{s^2} = (f^P,g^P)_p + (f^{H_>},g^{H_>})_h + (f^{H_<},g^{H_<})_h, \tag{6.18a}$$

$$(a,b)_p = \int_0^{\pi/2} d\theta\, a(\theta)^* b(\theta), \tag{6.18b}$$

$$(a,b)_h = \int_0^{\infty} d\theta\, a(\theta)^* b(\theta). \tag{6.18c}$$

Here again, $f^C(\theta)$ ($C = P^\sigma, H^\sigma_>, H^\sigma_<$) gives the three forms of a single function f over the support of the coupled state (i.e., the line $\sigma_1 r_1^2 + \sigma_2 r_2^2 = \sigma r^2$ in Fig. 2). The inner product $(\cdot,\cdot)_{s^2}$ will thus in general involve integration over more than one θ range.

6.10: In essence, the solution of Eqs. (6.14)–(6.18) is the solution of the Clebsch–Gordan problem for so(2,1), for once the proper $F^C_{k,\tau}(\theta)$ are found, the CGC's are obtained as the inner product between the coupled states (6.11) and the product states (6.3). The latter have support on a single point in the plane $\mathscr{S}^2$ of Fig. 2, which due to (6.5) lies on the line support of the coupled state. The CGC's are thus

$$C\begin{pmatrix}k_1, & k_2 & ;k\\ \tau_1,\rho_1, & \tau_2,\rho_2 & ;\tau\rho\end{pmatrix} = (\psi^{k_1,k_2}_{\tau_1,\rho_1,\tau_2,\rho_2}, \Psi^{k_1,k_2}_{k,\tau,\rho})_{\mathscr{S}^2}$$
$$= \delta(\tau_1\rho_1^2/2 + \tau_2\rho_2^2/2 - \tau\rho^2/2)(\rho_1\rho_2)^{-1/2} F^C_{k,\tau}(T), \tag{6.19}$$

where C refers to the chart where $(\tau_1,\rho_1,\tau_2,\rho_2)$ lies, according to (6.8a), and T is then given by

$$P^\tau\text{-chart:} \quad T = \arcsin(\rho_2/\rho) = \arccos(\rho_1/\rho), \tag{6.20a}$$

$$H^\tau_>\text{-chart:} \quad T = \operatorname{arcsinh}(\rho_2/\rho) = \operatorname{arccosh}(\rho_1/\rho), \tag{6.20b}$$

$$H^\tau_<\text{-chart:} \quad T = \operatorname{arccosh}(\rho_2/\rho) = \operatorname{arcsinh}(\rho_1/\rho). \tag{6.20c}$$

6.11: One obvious symmetry relation between the CGC's comes from the automorphism $A = A_1A_2$, whose role is to invert all σ's. Because of the factors δ_{σ_j,τ_j} and $\delta_{\sigma,\tau}$ in (6.3) and (6.11) and the unitarity of A under (6.10), it follows that

$$C\begin{pmatrix}k_1, & k_2 & ;k\\ \tau_1,\rho_1, & \tau_2,\rho_2 & ;\tau,\rho\end{pmatrix} = C\begin{pmatrix}k_1, & k_2 & ;k\\ -\tau_1,\rho_1, & -\tau_2,\rho_2, & ;-\tau,\rho\end{pmatrix} \tag{6.21}$$

for all SAIR couplings. A special case of this symmetry was noted in (4.13). We shall henceforth reduce ourselves to the calculation of CGC's inequivalent under this relation.

VII. THE COUPLING $D^+ \times D^+$

The coupling of two lower-bound (or upper-bound) discrete-series SAIR's into a direct sum of representations of the same type, constitutes the simplest application of the general method outlined in the preceding section.

7.1: Given the range of the $\mathscr{S}^2$ variables ($\sigma_1 = 1, \sigma_2 = 1$ and hence $\sigma = 1$) the coupled function $F_{k,\tau}(\theta)$ in (6.11) will have support only in the P^+-chart (6.8a). For $k_j \geqslant 1$, in the D^+ SAIR's outside the exceptional interval the Pöschl–Teller potential Schrödinger equation (Fig. 3) exhibits strong barriers at the interval ends, and the square-integrable solutions to (6.12a) are $w^{k_1,k_2,k}_{1(0)}(\theta)$ [Eq. (6.14a)] and $w^{k_1,k_2,k}_{1(1)}(\theta)$ [Eq. (6.15a)] at each of the P-chart endpoints. They represent the same solution only when $-k_1 - k_2 + k$ is zero or a positive integer, and this determines through (6.6) that only discrete-series SAIR's appear in the reduction of $D^+_{k_1} \times D^+_{k_2}$. The hypergeometric function in the solution is a polynomial in $\sin^2\theta$, and is easily converted into a Jacobi polynomial (Ref. 19, Eq. 15.4.6) $P^{(2k_2-1,2k_1-1)}_{k-k_1-k_2}(\cos 2\theta)$, multiplied by powers of $\cos\theta$ and $\sin\theta$ as required to provide an orthogonal set of solutions.

When k_1 and/or k_2 lie on the exceptional interval (0,1), the strong barrier at $\theta = \pi/2$ and/or 0 becomes a weak barrier/well, and any linear combination of $w^{k_1,k_2,k}_{1(N)}(\theta)$ and $w^{k_1,k_2,k}_{2(N)}(\theta)$ [N indicating the end point at which such a weak singularity occurs] would provide square-integrable solutions, thereby destroying the unique quantization of k. Equation (6.6), however, fixes the self-adjoint extension of the operators and hence the spectrum of the Pöschl–Teller Schrödinger equation to $k = k_1 + k_2 + n$, $n \in Z^+$. For all $k > 0$, hence, the solution vanishes at the end points, and its derivative is square integrable. The proper normalization constants for the solutions are easily found (Ref. 19, Eq. 22.2.1), and the rest of the program proceeds through (6.19) and (6.20a).

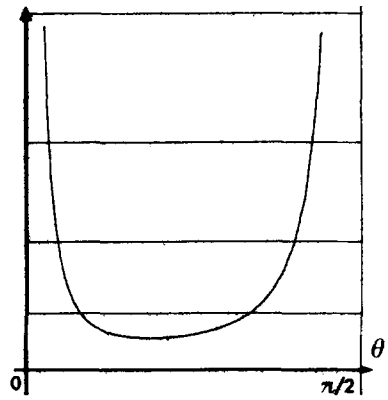

FIG. 3. Pöschl–Teller potential of the first kind for the coupling of $D^+ \times D^+$. The "energy levels" represent the direct summands in the product.

7.2: The CGC's for $D^+ \times D^+ \to D^+$ can be thus written as

$$C\begin{pmatrix} k_1, & k_2 & ; k \\ +1,\rho_1, & +1,\rho_2; & +1,\rho \end{pmatrix} = \delta(\rho_1^2/2 + \rho_2^2/2 - \rho^2/2)\, p_k^{k_1,k_2} \rho_1^{2k_1-1} \rho_2^{2k_2-1} \rho^{1-2k_1-2k_2} P^{(2k_2-1,2k_1-1)}_{k-k_1-k_2}([\rho_1^2 - \rho_2^2]/\rho^2)$$

$$= \delta(\rho_1^2/2 + \rho_2^2/2 - \rho^2/2)\, c_k^{k_1,k_2} \rho_1^{2k_1-1} \rho_2^{2k_2-1} \rho^{1-2k_1-2k_2} F\left[\begin{matrix} k_1+k_2-k, k_1+k_2+k-1 \\ 2k_2 \end{matrix}; \rho_2^2/\rho^2\right], \tag{7.1a}$$

where the normalization coefficients are

$$p_k^{k_1,k_2} = \left[\frac{2(2k-1)\Gamma(k_1+k_2+k-1)\Gamma(-k_1-k_2+k+1)}{\Gamma(k_1-k_2+k)\Gamma(-k_1+k_2+k)}\right]^{1/2}, \tag{7.1b}$$

$$c_k^{k_1,k_2} = \frac{1}{\Gamma(2k_2)}\left[\frac{2(2k-1)\Gamma(-k_1+k_2+k)\Gamma(k_1+k_2+k-1)}{\Gamma(k_1-k_2+k)\Gamma(-k_1-k_2+k+1)}\right]^{1/2}, \tag{7.1c}$$

and where the range of the coupled SAIR's is

$$k = k_1 + k_2 + n, \quad n \in Z^+. \tag{7.1d}$$

Note that if we set k_1 and k_2 to be $\frac{1}{4}$ or $\frac{3}{4}$, we obtain the $D^+_\circ \times D^+_\circ$ coupling coefficients (2.18).

For the $D^- \times D^-$ coupling the developments are the same, except that now $\sigma_1 = -1 = \sigma_2$ and hence $\sigma = -1$, so we are in the P^--chart. Through (6.21) we obtain CGC's identical to the above ones.

VIII. THE COUPLING $D^+ \times D^-$

The coupling of a positive and a negative discrete SAIR follows the general pattern of Sec. III. Here, the decomposition yields a direct integral of continuous nonexceptional representations plus, depending on whether $k_1 > k_2$ or $k_1 < k_2$, a finite sum of positive or negative discrete-series SAIR's.

8.1: As now $\sigma_1 = +1$ and $\sigma_2 = -1$ we have functions with support on the lower-right quadrant of Fig. 2, i.e., on the union of the $H^+_>$ and $H^-_<$ coordinate charts. Furthermore, depending on whether $\rho_1 > \rho_2$ or $\rho_1 < \rho_2$, the support lies entirely within one or the other. We have thus to satisfy Eqs. (6.12b) or (6.12c) separately. These are two Schrödinger equations for Pöschl–Teller potentials of the second kind, shown in Fig. 4. The singularity coefficient at the origin of the equation belonging to the $\sigma = +1$ chart depends on k_2, and that of the $\sigma = -1$ chart, on k_1. When $k_j > 1$, as in the

figures, the potential has a strong barrier at the origin. When one or both k_j lie on the exceptional interval, one or both of the two equations will present a weak barrier/well at the origin. In every case, a continuum of "free" generalized eigenfunctions exists.

When $k_1 > k_2 > \frac{3}{4}$ (Fig. 4), there is a minimum in the $\sigma = +1$ chart potential. When this happens, the quantum system exhibits a finite number of bound states. When either $k_2 < \frac{3}{4}$ (for $\sigma = +1$) or $k_1 < \frac{3}{4}$ (for $\sigma = -1$), the minimum shifts into the weak well at the origin, which continues, nevertheless, to have a finite number of bound states. The "negative-energy" bound states correspond to discrete-series coupled functions since their eigenvalue under J_-, i.e., $\sigma\rho^2/2$, is purely positive ($k_1 > k_2$) or purely negative ($k_1 < k_2$), telling us they belong to the D_k^+ or D_k^- SAIR's respectively. When $k_1 = k_2$, the $H_>^+$ and $H_<^-$ chart equations are identical. No minima exist. In the continuum, the "energy" eigenvalue in (6.8b) and (6.8c) is positive, i.e., $-(2k-1)^2 \geqslant 0$ so that the coupled states built with these solutions belong to the continuous nonexceptional series $k = (1 + i\kappa)/2$, $\kappa > 0$. The zero eigenvalue will be subject to further scrutiny.

8.2: We begin with the coupling to the continuous series in the $H_>^+$ chart, $\rho_1 > \rho_2$. The solutions $w_{1(0)}^{k_1,k_2,k}(\theta)$ in (6.13b)–(6.14a) are the appropriate ones, for they vanish at the origin when $k_2 \geqslant 1$ and have locally $\mathscr{L}^2$ derivatives when k_2 lies in the exceptional interval, as required by the function domain of the operators. Since these solutions oscillate at infinity, the Dirac-normalization constant may be obtained through a process parallel to (4.9), so that (6.17) may be satisfied. The rest of the program follows through (6.19) and (6.20b).

The CGC's for the $D^+ \times D^- \to C$ coupling are thus

$$C_> \begin{pmatrix} k_1, & k_2 & ;\epsilon k \\ +1,\rho_1, & -1,\rho_2; & +1,\rho \end{pmatrix} = \delta(\rho_1^2/2 - \rho_2^2/2 - \rho^2/2) \times c_k^{k_1,k_2} \rho_1^{2k_1-1} \rho_2^{2k_2-2} \rho^{1-2k_1-2k_2} \times F\left[\begin{matrix} k_1+k_2-k, k_1+k_2+k-1 \\ 2k_2 \end{matrix} ; -\rho_2^2/\rho^2 \right], \quad (8.1a)$$

where we have indicated that $\rho_1 > \rho_2$ through the ">" subindex, which will be henceforth used for similar cases, and where

$$c_k^{k_1,k_2} = [\pi\Gamma(2k_2)]^{-1} \times [\kappa \sinh \pi\kappa \Gamma(k_1+k_2-k)\Gamma(-k_1+k_2+k) \times \Gamma(k_1+k_2+k-1)\Gamma(-k_1+k_2-k+1)]^{1/2}. \quad (8.1b)$$

As usual, we have used $k = (1 + i\kappa)/2$ and we imply that

$$\epsilon \equiv \epsilon_1 + \epsilon_2 \equiv k_1 - k_2 \pmod 1. \quad (8.2)$$

We remind the reader that, for the discrete series, as detailed in Sec. VI, $\epsilon_1 \equiv k_1 \pmod 1$ in $D_{k_1}^+$ and $\epsilon_2 \equiv -k_2 \pmod 1$ in $D_{k_2}^-$. The sign is irrelevant only when the ϵ_j's are 0 and/or $\frac{1}{2}$. Finally, if we set $k_1, k_2 = \frac{1}{4}$ or $\frac{3}{4}$ in (8.1), we reproduce exactly the CGC's for the coupling of two oscillator representations given in (4.11).

When $\rho_1 < \rho_2$ we are in the $H_<^-$-chart with $\sigma = -1$. This case leads to a similar differential equation—(6.12b) vs (6.12c)— with k_1 and k_2 exchanged, as well as ρ_1 and ρ_2—(6.13b) vs (6.13c)—in all the ensuing developments. We thus find immediately

$$C_< \begin{pmatrix} k_1, & k_2 & ;\epsilon k \\ +1,\rho_1, & -1,\rho_2; & -1,\rho \end{pmatrix} = C_> \begin{pmatrix} k_2, & k_1 & ;\epsilon k \\ +1,\rho_2, & -1,\rho_1; & +1,\rho \end{pmatrix}. \quad (8.3)$$

8.3: We turn finally to the discrete series present in the decomposition of $D^+ \times D^-$. Consider first $k_1 > k_2$, when the potential has a minimum in the $H_>^+$-chart, as in Fig. 4(a). There is a unique self-adjoint extension of the operator in (6.12b) determined by (8.2) and, consequently, unique quantization. Analysis of the asymptotic form of the solution in (6.13b)–(6.14a) shows that $w_{1(0)}^{k_1,k_2,k}(\theta)$ decays exponentially for $k = k_1 - k_2, k_1 - k_2 - 1, \cdots > \frac{1}{2}$ (i.e., down to 1 or $\frac{3}{2}$ when $k_1 - k_2$ is an integer or half-integer). When $k = \frac{1}{2}$ (i.e., for $k_1 - k_2$ half-integer) $w_{1(0)}^{k_1,k_2,k}(\theta)$ tends asymptotically to a constant and hence is not in $\mathscr{L}^2(R^+)$. We conclude that a finite number of discrete representations occur for this range of values of k. Since $\sigma = +1$ in the $H_>^+$-chart, and no corresponding bound states appear for $\sigma = -1$ in the $H_<^-$-chart, we confirm (8.2) in that the representations belong to the D^+-series. The bound and free states in the $H_>^+$-chart are orthogonal. A Kummer transformation on (6.13b)–(6.14a) for $k - k_1 + k_2 = -n$, $n \in Z^+$, informs us that the hypergeometric function is a Jacobi polynomial of degree n in $-\sinh^2\theta$, $\theta \in [0, \infty)$. We may use Bargmann's hint [Ref. 1, Eq. (10.26)] to evaluate the proper normalization coefficient and finally express the resulting series in terms of a Jacobi polynomial in $1 - 2\tanh\theta \in [-1, 1]$. We follow with (6.19) and (6.20b).

The CGC's for the $D^+ \times D^- \to D^+$ coupling are thus

$$C_v \begin{pmatrix} k_1, & k_2 & ;k \\ +1,\rho_1, & -1,\rho_2; & +1,\rho \end{pmatrix} = \delta(\rho_1^2/2 - \rho_2^2/2 - \rho^2/2) p_k^{k_1,k_2} \rho_1^{-k_1-k_2-k+1} \rho_2^{2k_2-1} \rho^{k_1-k_2+k-1} P_{k_1-k_2-k}^{2k_2-1,2k-1}([\rho^2 - \rho_2^2]/\rho_1^2)$$

$$= \delta(\rho_1^2/2 - \rho_2^2/2 - \rho^2/2) c_k^{k_1,k_2} \rho_1^{-2k_1+1} \rho_2^{2k_2-1} \rho^{2k_1-2k_2-1} F\left[\begin{matrix} -k_1+k_2+k, -k_1+k_2-k+1 \\ 2k_2 \end{matrix} ; -\rho_2^2/\rho^2 \right], \quad (8.4a)$$

$$p_k^{k_1,k_2} = \left[\frac{2(2k-1)\Gamma(k_1+k_2+k-1)\Gamma(k_1-k_2-k+1)}{\Gamma(k_1+k_2-k)\Gamma(k_1-k_2+k)} \right]^{1/2}, \quad (8.4b)$$

$$c_k^{k_1,k_2} = \frac{1}{\Gamma(2k_2)} \left[\frac{2(2k-1)\Gamma(k_1+k_2-k)\Gamma(k_1+k_2+k-1)}{\Gamma(k_1-k_2+k)\Gamma(k_1-k_2-k+1)} \right]^{1/2}, \quad (8.4c)$$

$$k = k_1 - k_2, k_1 - k_2 - 1, \cdots > \tfrac{1}{2}. \quad (8.4d)$$

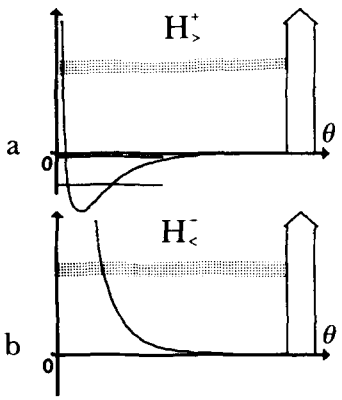

FIG. 4. Pöschl–Teller potentials of the second kind representing the coupling $D^+ \times D^-$ in (a) the $H^+_>$ chart and (b) the $H^-_<$ chart. The arrows indicate the coupling to the continuous series, while the discrete levels in (a) indicate the discrete-series summands in the coupling (a finite set).

The powers and hypergeometric function in (8.4a) and (8.1a) are the same, as can be seen through a Kummer transformation. The normalization coefficients are different, however.

When $k_1 < k_2$, the "bound states" appear in the $H^-_<$-chart, with $\sigma = -1$, and the same arguments which we used for (8.3) apply here. We thus conclude that the D^-_k SAIR's occur with CGC's related to the above through

$$C_< \begin{pmatrix} k_1, & k_2 & ;k \\ +1,\rho_1, & -1,\rho_2; & -1,\rho \end{pmatrix} = C_> \begin{pmatrix} k_2, & k_1 & ;k \\ +1,\rho_2, & -1,\rho_1; & +1,\rho \end{pmatrix}, \quad k_1 < k_2. \tag{8.5}$$

8.4: We would like to clarify now the appearance of the $k = \frac{1}{2}$ SAIR's in the $D^+ \times D^-$ coupling. They did not appear, we saw, among the "bound states" producing (8.4). The normalization coefficient (8.1b) appears to be zero when $k = (1 + i\kappa)/2$, $\kappa \to 0$; there is a cancelling pole, however, when either $k_1 + k_2 = \frac{1}{2}$ or when $k_1 - k_2 = \frac{1}{2}$ [the $k_1 - k_2 = -\frac{1}{2}$ case appears through (8.3)]. The former case applied to both σ-charts exhibiting $\epsilon \equiv \epsilon_1 + \epsilon_2 \equiv k_1 - k_2 \pmod 1$, $\epsilon \in (-\frac{1}{2}, \frac{1}{2})$, while the latter cases exhibit $\epsilon = \frac{1}{2}$ for $\sigma = +1$ only and $\epsilon = -\frac{1}{2}$ for $\sigma = -1$ only. Hence $k_1 + k_2 = \frac{1}{2}$ represents a nonzero coupling to the continuous series $C^{\epsilon}_{1/4}$ for $\epsilon \in (-\frac{1}{2}, \frac{1}{2})$ (belonging to the continuum of Fig. 4), while $k_1 - k_2 = \frac{1}{2}$, a coupling to $D^+_{1/2}$ belonging to the discrete series. The latter appeared, we recall, in $D^+_\circ \times D^-_\circ$ of Sec. IV.

IX. THE COUPLING $\mathscr{D} \times \mathscr{C}$

The analysis of the coupling of one discrete- and one continuous-series representation requires a more careful analysis: it involves three of the charts in Fig. 2, two of them joined as described briefly in Sec. VI.

9.1: We analyze first the $D^+ \times \mathscr{C}$ case, where $\sigma_1 = +1$ and $\sigma_2 = \pm 1$, so the relevant portion of Fig. 2 is the right half-plane constituted by the P^+-, $H^+_>$-, and $H^-_<$-charts. The $r_1 = 0$ axis carries a strong potential barrier (for $k_1 \geqslant 1$) or a weak barrier/well (for $0 < k_1 < 1$) in the associated Pöschl–Teller potentials; the $r_2 = 0$ axis carries a similar singularity depending on k_2: a strong well for $k_2 \in C$ and a weak barrier/well for $k_2 \in E$.

As described in Sec. VI solutions in the P^+- and $H^+_>$-charts must join through the cancellation of the boundary Wronskians, while the solutions in the $H^-_<$-chart remain disconnected, as shown in Fig. 5.

9.2: We treat first the latter case [Fig. 5(a), where the $H^-_<$ coordinates are (6.8c), the inner product is (6.10c), and the Pöschl–Teller potential is (6.12c), exhibiting only "free-state" solutions $w^{k_1,k_2,k}_{1(0)}(\theta)$ given by positive $-(2k-2)^2 > 0$, which represent couplings to the C-series and vanish, or are locally $\mathscr{L}^2$ at the origin]. These elements and boundary conditions were present in the derivation of the $D^+ \times D^-$ coupling in the same $H^-_<$-chart, in the last section. The result, Eq. (8.3), yields the $D^+ \times \mathscr{C} \to C$ CGC's, which we write explicitly as

$$C_< \begin{pmatrix} k_1, & \epsilon_2, k_2 & ;\epsilon, k \\ +1,\rho_1, & -1,\rho_2; & -1,\rho \end{pmatrix} = \delta(\rho_1^2/2 - \rho_2^2/2 + \rho^2/2) \times c_k^{k_1,k_2} \rho_1^{2k_1 - 1} \rho_2^{2k_2 - 1} \rho^{-2k_1 - 2k_2 + 1} \times F\left[\begin{matrix} k_1 + k_2 - k, k_1 + k_2 + k - 1 \\ 2k_1 \end{matrix} ; -\rho_1^2/\rho^2 \right], \tag{9.1a}$$

$$c_k^{k_1,k_2} = [\pi \Gamma(2k_1)]^{-1} [\kappa \sinh \pi\kappa \times \Gamma(k_1 + k_2 - k)\Gamma(k_1 - k_2 + k)\Gamma(k_1 + k_2 + k - 1) \times \Gamma(k_1 - k_2 - k + 1)]^{1/2}, \tag{9.1b}$$

$$\epsilon \equiv \epsilon_1 + \epsilon_2 \equiv k_1 + \epsilon_2 \pmod 1, \tag{9.1c}$$

where again $k = (1 + i\kappa)/2$, but with the addendum that $k_2 = (1 + i\kappa_2)/2$ for $k_2 \in C$ or $k_2 = (1 + \kappa_2)/2, 0 < \kappa_2 < 1$ for $k_2 \in E$ [thus ϵ_2 in (9.1c) replaces k_2 in (8.2c).] The normalization coefficient (9.1b) is, of course, real.

9.3: The new feature which the $\mathscr{D} \times \mathscr{C}$ coupling introduces over previous cases is the form of the solution in the $\sigma = +1$ region, constituted by the union of the P^+- and $H^+_>$-charts. The inner product will contain the first two summands in (6.10a), where the coupled states will have one form in each chart, eigenfunctions of the Casimir operator, itself having forms (6.9a) and (6.9b) in each of the two charts,

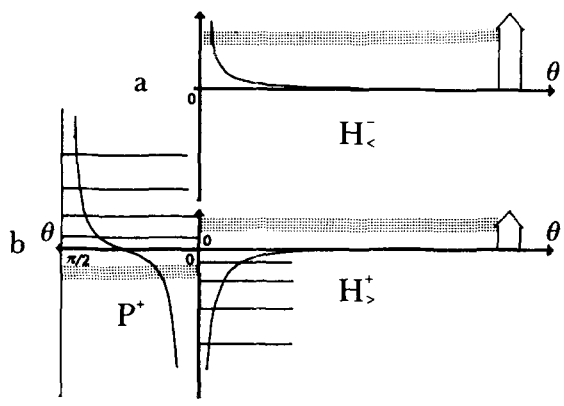

FIG. 5. The $\mathscr{D} \times \mathscr{C}$ coupling in (a) the $H^-_<$ chart and (b) in the region composed of the P^+ and $H^+_>$ charts. The former contains only coupling to the continuous series, while the latter includes both continuous and discrete series.

with a single eigenvalue $k(1-k)$.

The two Pöschl–Teller potentials are shown in Fig. 5(b). They do not join, but the two parts of the figure have only been placed so that the boundary Wronskians at adjacent points are indicated to cancel [see Eq. (9.4) ahead]. We shall consider first the $D^+\times\mathscr{C}\to D^+$ coupling to the discrete series, which corresponds to bound ("negative-energy") states in the $H_>^+$-chart potential, joined with a "positive-energy" state in the P^+-chart potential, due to the difference in the sign of the right-hand side of (6.12). The barrier due to the $D_{k_1}^+$ factor closes the system from the left, while on the right the potential rises exponentially to zero. A strong well or weak barrier/well due to the $C_{q_2}^{\epsilon}$ factor lies at the join of the two regions. The cases when k_1 and/or k_2 lie in the exceptional interval are important, but constitute minor modifications of the basic construction. In the $H_>^+$-chart, the rising potential imposes one constraint and reduces the solution there to be $f_k^{H_>}(\theta)=C_k^{H_>}w_{2(\infty)}^{k_1,k_2,k}(\theta)$, with an as yet undetermined constant $C_k^{H_>}$. A second constraint in the P^+-chart comes from square-integrability at $\theta_P=0$, and similarly for the derivative, reducing the solution there to $f_k^P(\theta)=C_k^P w_{1(1)}^{k_1,k_2,k}(\theta)$, with another constant C_k^P.

The inner product (6.18) of such two-chart functions, corresponding to eigenvalues $k(1-k)$ and $l(1-l)$ can be evaluated, as was done in (5.8), in terms of the boundary Wronskians:

$$\begin{aligned}(f_k,f_l)_{s^2}&=(f_k^P,f_l^P)_P+(f_k^{H_>},f_l^{H_>})_h\\&=[4(k+l-1)(l-k)]^{-1}\big[C_k^{P*}C_l^P W(w_{1(1)}^{k*}mw_{1(1)}^{l})\,|_0^{\pi/2}\\&\quad-C_k^{H_>*}C_l^{H_>}W(w_{2(\infty)}^{k*},w_{2(\infty)}^{l})\,|_0^{\infty}\big].\end{aligned}\tag{9.2}$$

This expression should equal $\delta_{k,l}$, and thus it must be zero for $k\neq l$; the two nonzero boundary values at $\theta_P=0$ and $\theta_{H_>}=0$ must therefore be equal in order to cancel. The relative minus sign between the Wronskians is due to the sign difference in the eigenvalue in (6.12). Since (Ref. 19, Eq. 15.3.6)

$$w_{1(1)}^{k_1,k_2,k}(\theta)=A_k w_{1(0)}^{k_1,k_2,k}(\theta)+\tilde{A}_k w_{2(0)}^{k_1,k_2,k}(\theta),\tag{9.3a}$$

$$\begin{aligned}A_k&=\Gamma(2k_1)\Gamma(-2k_2+1)/\Gamma(k_1-k_2+k)\\&\quad\times\Gamma(k_1-k_2-k+1),\\\tilde{A}_k&=A_k(k_2\leftrightarrow 1-k_2),\end{aligned}\tag{9.3b}$$

and (Ref. 19, Eq. 15.3.7)

$$w_{2(\infty)}^{k_1,k_2,k}(\theta)=B_k w_{1(0)}^{k_1,k_2,k}(\theta)+\tilde{B}_k w_{2(0)}^{k_1,k_2,k}(\theta),\tag{9.4a}$$

$$\begin{aligned}B_k&=\Gamma(2k)\Gamma(-2k_2+1)/\Gamma(k_1-k_2+k)\\&\quad\times\Gamma(-k_1-k_2+k+1),\\\tilde{B}_k&=B_k(k_2\leftrightarrow 1-k_2),\end{aligned}\tag{9.4b}$$

we may evaluate the boundary Wronskians explicitly. We note that for $k_2\in C$ the two summands in (8.3a) are complex conjugates, and similarly in (8.4a), while for $k\in E$ they are all real. One obtains thus

$$W(w_{1(1)}^{k*},w_{1(1)}^{l})|_{\theta_P\to 0^+}=2(2k_2-1)(\tilde{A}_k A_l-A_k\tilde{A}_l),\tag{9.5a}$$

$$W(w_{2(\infty)}^{k*},w_{2(\infty)}^{l})\,|_{\theta_{H_>}\to 0^+}=2(2k_2-1)(\tilde{B}_k B_l-B_k\tilde{B}_l).\tag{9.5b}$$

When the ratio of the latter two is asked to factor into $(C_k^P/C_k^{H_>})^*(C_l^P/C_l^{H_>})$, one finds that this does not generally happen. The requirement may be imposed only when $k-l$ is an integer. The domain restriction (9.1c) implies then that $k=\epsilon,\epsilon+1,\epsilon+2,\cdots$ and similarly for l. Hence, one finds

$$\begin{aligned}C_k^P/C_k^{H_>}&=\pi^{-1}[\sin\pi(k_2+\epsilon_2)\sin\pi(k_2-\epsilon_2)]^{1/2}\\&\quad\times\Gamma(2k_1)^{-1}\Gamma(2k)\Gamma(k_1+k_2-k)\\&\quad\times\Gamma(k_1-k_2-k+1).\end{aligned}\tag{9.6}$$

From (9.1c), this ratio is real. We also note the close resemblance between the radicands in (9.6) and in (5.9). Indeed, it tells us that when $k_2\in E$ is such that $\pm\epsilon_2\to k_2$, the ratio (9.3) develops a zero or a pole, so that the P- and $H_>$-function pieces become independent and reduce each to the $D^+\times D^+$ or $D^+\times D^-$ couplings seen in Secs. VII and VIII.

The last step is to normalize the function f_k so that $(f_k,f_k)_{s^2}=1$. This is done on (9.2) in the manner of (3.14), which essentially reduces to obtaining the derivative of the two boundary terms with respect to l and valuate at $l=k$. (The boundary terms cancel for $k-l$ integer, but lead separate lives for all other $l-k$; hence the derivative of the boundary term difference is not zero.) The resulting ψ functions combine to form trigonometric ones, and the result simplifies drastically. Use of (6.20a) or (6.20b) for the corresponding chart leads to the CGC's as in (6.19).

The CGC's for the $D^+\times\mathscr{C}\to D^+$ coupling are thus

$$C\begin{pmatrix}k_1, & \epsilon_2,k_2 & ;k\\ +1,\rho_1, & +1,\rho_2; & +1,\rho\end{pmatrix}=\delta(\rho_1^2/2+\rho_2^2/2-\rho^2/2)\times c_{k,P}^{k_1,k_2}\rho_1^{2k_1-1}\rho_2^{2k_2-1}\rho^{-2k_1-2k_2+1}F\left[\begin{matrix}k_1+k_2-k,k_1+k_2+k-1\\ 2k_1\end{matrix};\rho_1^2/\rho^2\right],\tag{9.7a}$$

$$c_{k,P}^{k_1,k_2}=\frac{1}{\Gamma(2k_1)}\left[\frac{2(2k-1)\Gamma(k_1-k_2+k)\Gamma(k_1+k_2+k-1)}{\Gamma(-k_1+k_2+k)\Gamma(-k_1-k_2+k+1)}\right]^{+1/2},\tag{9.7b}$$

and

$$C_>\begin{pmatrix}k_1, & \epsilon_2,k_2 & ;k\\ +1,\rho_1, & -1,\rho_2; & +1,\rho\end{pmatrix}=\delta(\rho_1^2/2-\rho_2^2/2-\rho^2/2)\times c_{k,H}^{k_1,k_2}\rho_1^{-2k_1+1}\rho_2^{2k_1-2k-1}\rho^{2k-1}F\left[\begin{matrix}-k_1+k_2+k,-k_1-k_2+k+1\\ 2k\end{matrix};-\rho_2^2/\rho^2\right],\tag{9.8a}$$

$$c_{k,H}^{k_1,k_2}=\frac{1}{\Gamma(2k)}\left[\frac{2(2k-1)\Gamma(k_1-k_2+k)\Gamma(k_1+k_2+k-1)}{\Gamma(k_1+k_2-k)\Gamma(k_1-k_2-k+1)}\right]^{1/2},\tag{9.8b}$$

where it is implied that (8.1c) holds, and the subscript " $>$ " of the CGC menas that $\rho_1 > \rho_2$.

9.4: It should be noted that for $\frac{3}{4} > k_2 > 1$ the Casimir operator Q has a negative spectrum $k(1-k)$ and nonvanishing "wavefunctions," even though the Pöschl–Teller potential in the $H^+_>$-chart [Fig. 5(b)] is purely positive. Of course, the joined P^+-chart must also be considered, but this remark only underlines the fact that a physicist's intuition on Schrödinger equation solutions may go astray for two- and three-chart such operators.

In contradistinction to the matching of solutions in Schrödinger equations with finite discontinuous potentials, where the two sides of a single wavefunction and its derivative across the discontinuity are made equal, here we must only cancel the boundary Wronskians of a pair of functions on two charts. The functions themselves at $\theta \to 0^+$ behave as $A_k \theta^{1/2+i\kappa_2} + \tilde{A}_k \theta^{1/2-i\kappa_2}$, $i\kappa_2 = 2k_2 - 1$. They are real, tend to zero, but their derivative is not defined at the boundary. The boundary is thus not simply a point where the potential has a discontinuity/singularity as Figs. 2 and 5(b) might suggest at first sight.

9.5: We now examine the next case: the $D^+ \times \mathscr{C} \to C$ coupling to a continuous-series representation. The proper function on the P^+-chart continues to be $w^{k_1,k_2,k}_{1(1)}(\theta)$, with boundary Wronskian (9.5a). In the $H^+_>$-chart, however, we may have any linear combination of $w^{k_1,k_2,k}_{1(\infty)}(\theta)$ and $w^{k_1,k_2,k}_{2(\infty)}(\theta)$; the former behaves asymptotically as $\exp(i\kappa\theta)$ and the latter as $\exp(-i\kappa\theta)$. It can be verified that when the solution family is taken in the linear combination

$$f^{H_>}_k(\theta) = C_k w^{k_1,k_2,k}_{1(\infty)}(\theta) + C^*_k w^{k_1,k_2,k}_{2(\infty)}(\theta), \quad C^*_k = C_{1-k} \tag{9.9a}$$

[the second summand being the complex conjugate of the first: see Eq. (6.16b)], the Wronskian of any pair of functions $f^{H_>}_k$, $f^{H_>}_l$ in the family behaves asymptotically as the Fourier transform Dirichlet kernel, representing $2\pi|C_k|^2 \times [\delta(\lambda-\kappa) + \delta(\lambda+k)]$. This is analogous to (4.9) and provides the Dirac normalization.

The cancellation of the pair's Wronskian at $\theta_{H_>} \to 0$ with the companion P-chart Wronskian (9.5a) over a continuous range of k and l requires that $f^{H_>}_k(\theta)$ have, in terms of solutions around zero, the real form

$$f^{H_>}_k(\theta) = \alpha A_k w^{k_1,k_2,k}_{1(0)}(\theta) + \alpha^{-1} \tilde{A}_k w^{k_1,k_2,k}_{2(0)}(\theta), \tag{9.9b}$$

with α an as-yet free parameter, independent of k, subject only to the restriction $|\alpha| = 1$ for $k_2 \in C$ and $\alpha = \alpha^*$ for $k_2 \in E$. This freedom is allowed since the boundary Wronskian [Eq. (9.5b) with $B_k \to \alpha A_k$ and $\tilde{B}_k \to \alpha^{-1}\tilde{A}_k$] is quadratic in the coefficients of (9.9b) and independent of α. We may write the coefficients C_k in (9.9a) in terms of those in (9.9b) through (Ref. 19, Eq. 15.3.7)

$$C_k = C^*_{1-k} = \frac{\Gamma(2k-1)\Gamma(2k_1)}{\Gamma(k_1-k_2+k)\Gamma(k_1+k_2+k-1)} \left[\frac{\sin\pi(k-k_1)}{\sin\pi k_2} \frac{\alpha+\alpha^{-1}}{2} + \frac{\cos\pi(k-k_1)}{\cos\pi k_2} \frac{\alpha-\alpha^{-1}}{2} \right]. \tag{9.10a}$$

The condition to fix α turns out to be the necessary orthogonality between the continuous-k "free" generalized eigenstates and the discrete-k "bound" eigenstates seen before. Indeed, the Wronskians of two functions, each in one family, at $\theta_P = 0$ and $\theta_{H_>} = 0$, cancel only when

$$\alpha = [\sin\pi(k_2-\epsilon_2)/\sin\pi(k_2+\epsilon_2)]^{1/2}. \tag{9.10b}$$

Replacing this into (9.10a) and taking (9.1c) into account, we find the proper normalization constants for the two-chart functions. Finally, we use (6.19) with (6.20a) and (6.20b) for the rest of the process.

The CGC's for the $D^+ \times \mathscr{C} \to C$ coupling are thus

$$C\begin{pmatrix} k_1, & \epsilon_2, k_2 & ; \epsilon, k \\ +1, \rho_1, & +1, \rho_2 & ; +1, \rho \end{pmatrix} = \delta(\rho_1^2/2 + \rho_2^2/2 - \rho^2/2) c^{k_1,k_2}_{k,P} \rho_1^{2k_1-1} \rho_2^{2k_2-1} \rho^{-2k_1-2k_2+1} \times F\left[\begin{matrix} k_1+k_2-k, k_1+k_2+k-1 \\ 2k_1 \end{matrix} ; \rho_1^2/\rho^2 \right], \tag{9.11a}$$

$$c^{k_1,k_2}_{k,P} = [\pi\Gamma(2k_1)]^{-1} [\tfrac{1}{2}\kappa \sinh\pi\kappa \Gamma(k_1+k_2-k)\Gamma(k_1-k_2+k)\Gamma(k_1+k_2+k-1)\Gamma(k_1-k_2-k+1)] \times \sin\pi(k_2+\epsilon_2)\sin\pi(k_2-\epsilon_2)/\sin\pi(k+\epsilon)\sin\pi(k-\epsilon)]^{1/2}, \tag{9.11b}$$

and

$$C_> \begin{pmatrix} k_1, & \epsilon_2, k_2 & ; \epsilon, k \\ +1, \rho_1, & -1, \rho_2 & ; +1, \rho \end{pmatrix} = \delta(\rho_1^2/2 - \rho_2^2/2 - \rho^2/2) \times \left\{ c^{k_1,k_2}_{k,H} \rho_1^{2k_1-1} \rho_2^{2k_2-1} \rho^{-2k_1-2k_2+1} F\left[\begin{matrix} k_1+k_2-k, k_1+k_2+k-1 \\ 2k_2 \end{matrix} ; -\rho_2^2/\rho^2 \right] + (k_2 \leftrightarrow 1-k_2) \right\}, \tag{9.12a}$$

$$c^{k_1,k_2}_{k,H} = (-1)^{k_1-\epsilon_1} \frac{\Gamma(2k-1)}{\pi} \left[\tfrac{1}{2}\kappa \sinh\pi\kappa \frac{\Gamma(k_1+k_2-k)\Gamma(k_1-k_2-k+1)}{\Gamma(k_1-k_2+k)\Gamma(k_1+k_2+k-1)} \frac{\sin\pi(k-\epsilon)}{\sin\pi(k+\epsilon)} \right]^{1/2}, \tag{9.12b}$$

where, again, (9.1c) is implied.

The expressions for the $\tau = 1$ CGC's follow from (6.21).

9.6: We have given in some detail the considerations which allowed the introduction of the parameter α in (9.9b). Some further remarks may place its origin in a different context: The CGC's are being found, basically, as the solutions

to a single differential equation [Eqs. (6.12)] written in terms of a single complex variable Θ [Eqs. (6.13)] along three line segments in the complex plane. The two-chart $D^+ \times \mathscr{C}$ coupling seen in this section requires the two segments $[0,\pi/2]$ and $[0,i\infty)$ which meet at $\Theta = 0$, at the common boundary suggested by Figs. 2 and 5(b). The potential barrier at $\Theta = \theta_P = \pi/2$ fixes the solution to be $w^{k_1,k_2,k}_{1(1)}(\Theta)$. If we take seriously the idea of analytic continuation of the solutions from one chart to another, through the L-shaped contour in the complex Θ-plane (thus automatically cancelling boundary Wronskians), the same $w^{k_1,k_2,k}_{1(1)}(\Theta)$ solution ought to continue into the $H_>$ region up along the contour. As was pointed out after Eqs. (6.14)–(6.16), however, $w^{k_1,k_2,k}_{1(1)}(\Theta)$, $\Theta \in iR^+$ lies along the branch cut of the hypergeometric function, namely $[1,\infty)$. Moreover, as a closer examination will reveal, although our solution (9.9) on the $H_>$-chart has the appropriate coefficients to reconstitute precisely $w^{k_1,k_2,k}_{1(1)}(i\theta)$, the relative constant phase factor is undetermined insofar as the Riemann sheet of the function is not specified. Finally, as one can again verify, if we choose any one Riemann sheet, the obtained $w^{k_1,k_2,k}_{1(1)}(i\theta)$ will not exhibit the appropriate asymptotic behavior (9.9a) to allow for Dirac orthonormalization of the function set. Through linear combinations of the functions on various sheets, nevertheless, we can produce this behavior. This freedom in the choice is equivalent to the introduction of the constant α in (9.9). We may conclude that this parametrized multivaluation of the two-chart Pöschl–Teller eigenfunctions is a feature associated with the branch cut of the Gauss hypergeometric function. The proper value of α was found in (9.10b) through the requirement of orthogonality between the discrete and continuous spectrum eigenfunctions.

These considerations will apply to all cases in the next section—involving three charts.

X. THE COUPLING $\mathscr{C} \times \mathscr{C}$

This section examines the coupling of two continuous series SAIR's to SAIR's belonging to the discrete, continuous and—if both factor SAIR's are exceptional—a single SAIR of the exceptional continuous series.

10.1: When two continuous-series SAIR's couple, as both σ_1 and σ_2 may be ± 1, all six charts of Fig. 2 enter into the picture; three of them in the upper-right half-plane for the total $\sigma = 1$, and three in the lower-left half-plane for total $\sigma = -1$. In each case, the $H_<$, P-, and $H_>$-charts involve strongly welled (and/or weakly barriered/welled) Pöschl–Teller potentials of the first and second kind, as shown in Fig. 6. The total Casimir operator eigenfunctions have three forms, one in each chart. Under the total inner product [Eqs. (6.18) with either $\sigma = +1$ or $\sigma = -1$] the solutions should be orthonormal, in the ordinary or generalized sense, according to whether the coupling is made into the $\mathscr{D}$ or $\mathscr{C}$ SAIR's, corresponding respectively to bound or free states of the H-chart potentials. Furthermore, they must be mutually orthogonal.

10.2: Again, we consider first the coupling $\mathscr{C} \times \mathscr{C} \to \mathscr{D}$ to the discrete series SAIR's, where $-(2k-1)^2 \leqslant 0$ correspond to the "bound" states of Fig. 6. The asymptotic behavior of a normalizable solution f_k must be the exponentially decreasing $w^{k_1,k_2,k}_{2(\infty)}(\theta_{H_>})$ in the $H_>$-chart, and similarly for the $H_<$-chart. Keeping (6.16c) in mind, we set

$$f^{H_>}_k(\theta) = C^{H_>}_k w^{k_1,k_2,k}_{2(\infty)}(\theta), \quad f^{H_<}_k(\theta) = C^{H_<}_k w^{k_2,k_1,k}_{2(\infty)}(\theta), \tag{10.1}$$

and leave $f^P_k(\theta)$ free and subject to adjustment so that, in

$$\begin{aligned}(f_k,f_l)_{s^2} &= (f^{H_<}_k, f^{H_<}_l)_h + (f^P_k, f^P_l)_p + (f^{H_>}_k, f^{H_>}_l)_h \\ &= [4(k+l-1)(k-l)]^{-1}\left[C^{H_<}_k {}^* C^{H_<}_l W(w^{k_2,k_1,k*}_{2(\infty)}, w^{k_2,k_1,l}_{2(\infty)})\,|^{\infty}_0\right. \\ &\quad \left. - W(f^{P*}_k, f^P_l)\,|^{\pi/2}_0 + C^{H_>}_k {}^* C^{H_>}_l W(w^{k_1,k_2,k*}_{2(\infty)}, w^{k_1,k_2,l}_{2(\infty)})\,|^{\infty}_0\right],\end{aligned} \tag{10.2}$$

the "adjoining" Wronskian boundary values [at $\theta_{H_<} = 0$, $\theta_P = \pi/2$ and at $\theta_P = 0$, $\theta_{H_>} = 0$, as suggested by Fig. 6] cancel. At $\theta_{H_<} \to \infty$ and $\theta_{H_>} \to \infty$ they vanish exponentially due to the solution choice.

The condition of pairwise Wronskian cancellation should provide the expression for $f^P_k(\theta)$ in terms of $w^{k_1,k_2,k}_{n(0)}(\theta)$ or of $w^{k_1,k_2,k}_{m(1)}(\theta)$, $n,m = 1,2$, the relative coefficient ratio among the solutions in the three charts, and the quantization condition ($k - l$ integer). It will be observed that the branch cut of the hypergeometric functions in $w^{k_1,k_2,k}_{n(\infty)}(\Theta)$, $n = 1,2$, as given by (5.16) now falls on the P-chart θ range. For this reason we may expect, as in the $\mathscr{D} \times \mathscr{C} \to \mathscr{C}$ case of the last section, certain multivaluation features for the solution functions in this interval.

We proceed as in the last section, exploring the behavior of the fixed functions $w^{k_1,k_2,k}_{2(\infty)}(\theta)$ near $\theta_{H_>} \to 0^+$. This is given by $B^{>}_k \theta^{2k_2 - 1/2} + \tilde{B}^{>}_k \theta^{-2k_2 + 3/2}$, where $B^{>}_k$ and $\tilde{B}^{>}_k = B^{>}_k(k_2 \leftrightarrow 1 - k_2)$ are found from the $z \leftrightarrow 1/z$ linear transformation formulas (Ref. 19, Eq. 15.3.7) between Gauss functions, and given in (9.4b) as B_k. When $k_2 \in C$, the second summand is the complex conjugate of the first, while when $k_2 \in E$ they are both real. The boundary Wronskian is given in (9.5b). A similar expression holds for the function in the $H_<$-chart, with k_1 and k_2 exchanged, and coefficients which we shall denote by $B^{<}_k = B^{>}_k$ $(k_1 \leftrightarrow k_2)$ and $\tilde{B}^{<}_k = B^{<}_k$ $(k_1 \leftrightarrow 1 - k)$. We may now write the general solution in P-chart as

$$\begin{aligned} f^P_k(\theta) &= \beta_k B^{>}_k w^{k_1,k_2,k}_{1(0)}(\theta) + \tilde{\beta}_k \tilde{B}^{>}_k w^{k_1,k_2,k}_{2(0)}(\theta) \\ &= \gamma_k B^{<}_k w^{k_1,k_2,k}_{1(1)}(\theta) + \tilde{\gamma}_k \tilde{B}^{<}_k w^{k_1,k_2,k}_{2(1)}(\theta), \end{aligned} \tag{10.3}$$

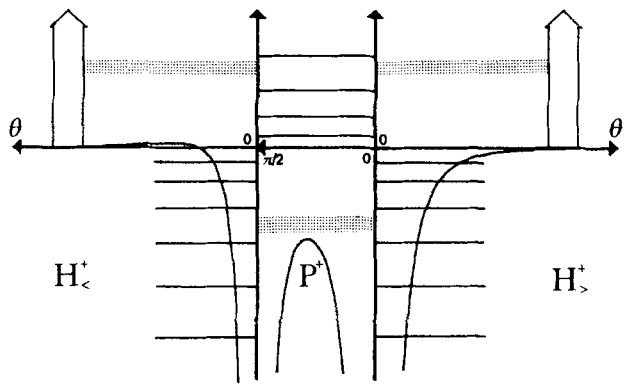

FIG. 6. The $\mathscr{C} \times \mathscr{C}$ coupling in the region composed of the $H^+_<$, P^+, and $H^+_>$ charts. Both continuous- and discrete-series summands are obtained.

which lead to real $f_k^{P}(\theta)$ when $\tilde{\beta}_k = \beta_k^*$ for $k_2 \in C$ or $\beta_k, \tilde{\beta}_k$ real for $k_2 \in E$. The expressions of $w^k_{m(0)}(\theta)$ in terms of the $w^{(k)}_{n(1)}(\theta)$ leads to the following relation between the γ's and the β's:

$$\gamma_k = [\sin 2\pi k_2]^{-1}[\beta_k \sin \pi(k_1 - k_2 + k) + \tilde{\beta}_k \sin \pi(k_1 + k_2 + k)], \tag{10.4}$$

and $\tilde{\gamma}_k$ given by the above expression exchanging $k_1 \leftrightarrow 1 - k_1$. For $k_1 \in C$, $\tilde{\gamma}_k = \gamma_k^*$ while for $k_1 \in E$ both γ_k and $\tilde{\gamma}_k$ are real, i.e., the γ's have the same properties as the β's only exchanging k_1 and k_2.

Now, the boundary value of $W(f_k^{P*}, f_l^{P})$ at $\theta_P \to 0^+$ may equal that of $W(w^{k*}_{2(\infty)}, w^{l}_{2(\infty)})$ at $\theta_{H_>} \to 0^+$ only when $\tilde{\beta}_k \beta_l = \beta_k \tilde{\beta}_l$ for all values of k and l in a discrete range. The normalization constants in (10.1) will then relate as $C_k^{H_>} = (\beta_k \tilde{\beta}_k)^{1/2}$. The same statement holds true at $\theta_P \to \pi/2^-$ and $\theta_{H_<} \to 0$: $\tilde{\gamma}_k \gamma_l = \gamma_k \tilde{\gamma}_l$ and $C_k^{H_<} = (\gamma_k \tilde{\gamma}_k)^{1/2}$. If the conditions on the β's and the γ's are to hold simultaneously, the relation (10.4) implies that $k - l$ must be an integer, i.e., $k = \epsilon + n$, $n \in Z^+$, are the allowed values of the spectrum, with $\epsilon \equiv \epsilon_1 + \epsilon_2 \pmod 1$ as given by (6.6). The overall normalization of the three-chart functions f_k, $k \in \mathscr{D}$, then follows from (10.1) upon letting $l \to k$, and reasoning in analogy with (3.14). It yields

$$(f_k, f_l)_{s^2} = [2(2k-1)]^{-1}[(2k_2 - 1)B_k^{\gtrless} \tilde{B}_k^{\gtrless} \beta_k \tilde{\beta}_k \partial_k \ln(\beta_k/\tilde{\beta}_k) + (2k_1 - 1)B_k^{\lessgtr} \tilde{B}_k^{\lessgtr} \gamma_k \tilde{\gamma}_k \partial_k \ln(\gamma_k/\tilde{\gamma}_k)]. \tag{10.5}$$

It should be noted that one choice of β's (and corresponding γ's) is

$$\left.\begin{aligned}\beta_k &= \sin \pi(k_2 + \epsilon_2)\\ \tilde{\beta}_k &= \sin \pi(k_2 - \epsilon_2)\end{aligned}\right\} \Leftrightarrow \begin{cases}\gamma_k = \sin \pi([k_1 + \epsilon_1] + [k - \epsilon])\\ \tilde{\gamma}_k = \sin \pi([k_1 - \epsilon_1] - [k - \epsilon]).\end{cases} \tag{10.6}$$

The required orthogonality of f_k, $k \in \mathscr{D}$, with f_l, $l \in \mathscr{C}$, as will be seen below, further restricts $\beta_k/\tilde{\beta}_k$ and $\gamma_k/\tilde{\gamma}_k$ to be constants independent of k (for $k = \epsilon + n$, $n \in Z^+$). The choice (10.6) turns out thus to be essentially unique—up to constants which are compensated by normalization—for the orthogonality of the full eigenfunction set.

Incorporating (10.6) into (10.5) and into the constants in (10.1a) and (10.3), we find the CGC's of the $\mathscr{C} \times \mathscr{C} \to D^+$ coupling through (6.15), (6.19), and (6.20). The results are, for the P-, $H_>$-, and $H_<$-charts,

$$C\begin{pmatrix}\epsilon_1,k_1, & \epsilon_2,k_2; & k\\ +1,\rho_1, & +1,\rho_2; & +1,\rho\end{pmatrix} = \delta(\rho_1^2/2 + \rho_2^2/2 - \rho^2/2) \times \left\{c_{k,P}^{k_1,k_2} \rho_1^{2k_1-1} \rho_2^{2k_2-1} \rho^{-2k_1-2k_2+1} F\left[\begin{matrix}k_1 + k_2 - k, k_1 + k_2 + k - 1\\ 2k_1\end{matrix}; \rho_1^2/\rho\right] + (k_1 \leftrightarrow 1 - k_1)\right\}, \tag{10.7a}$$

$$c_{k,P}^{k_1,k_2} = \frac{(-1)^{k-\epsilon}}{\pi} \sin \pi(k_1 + \epsilon_1) \Gamma(-2k_1 + 1)\left[\frac{2(2k-1)\Gamma(k_1 - k_2 + k)\Gamma(k_1 + k_2 + k - 1)}{\Gamma(-k_1 + k_2 + k)\Gamma(-k_1 - k_2 + k + 1)}\right]^{1/2}, \tag{10.7b}$$

$$C_>\begin{pmatrix}\epsilon_1,k_1, & \epsilon_2,k_2; & k\\ +1,\rho_1, & -1,\rho_2; & +1,\rho\end{pmatrix} = \delta(\rho_1^2/2 - \rho_2^2/2 - \rho^2/2) \times c_{k,H}^{k_1,k_2} \rho_1^{2k_1-1} \rho_2^{2k-2k+1} \rho^{2k-1} F\left[\begin{matrix}k_1 - k_2 + k, k_1 + k_2 + k - 1\\ 2k\end{matrix}; -\rho^2/\rho_2^2\right], \tag{10.8a}$$

$$c_{k,H}^{k_1,k_2} = [\pi\Gamma(2k)]^{-1}[2(2k-1)\sin\pi(k_2 + \epsilon_2)\sin\pi(k_2 - \epsilon_2) \times \Gamma(k_1 - k_2 + k)\Gamma(-k_1 + k_2 + k)\Gamma(k_1 + k_2 + k - 1)\Gamma(-k_1 - k_2 + k + 1)]^{1/2}, \tag{10.8b}$$

$$C_<\begin{pmatrix}\epsilon_1,k_1, & \epsilon_2,k_2; & k\\ -1,\rho_1, & +1,\rho_2; & +1,\rho\end{pmatrix} = C_>\begin{pmatrix}\epsilon_2,k_2, & \epsilon_1,k_1; & \epsilon,k\\ +1,\rho_2, & -1,\rho_1; & +1,\rho\end{pmatrix}, \tag{10.9}$$

where the subscript $\gtrless$ implies that $\rho_1 \gtrless \rho_2$.

The CGC's for the $\mathscr{C} \times \mathscr{C} \to D^-$ coupling are obtained through (6.21) from the above expressions.

10.3: There is one exceptional solution (10.1)–(10.3) which falls outside the limitations of our previous quantization of $k \in D$, and this is obtained when $B_k^{\gtrless} = 0 = B_k^{\lessgtr}$ due to a pole of one of the Γ functions in (9.4b) at the value

$$k = k_0 = k_1 + k_2 - 1. \tag{10.10}$$

This solution is hence present only when two exceptional continuous SAIR's are coupled to a total k. Since $\epsilon = \epsilon_1 + \epsilon_2$ is in general different from $\pm k_0$, we conclude that it belongs to the exceptional continuous type of SAIR's. It is thus only present when $\frac{1}{2} < k_0 < 1$, i.e., for $\frac{3}{2} < k_1 + k_2 < 2$ or, for $k_j = (1 + \kappa_j)/2$, $1 < \kappa_1 + \kappa_2 < 2$. In that case, $\tilde{B}_{k_0}^{\gtrless} = 1 = \tilde{B}_{k_0}^{\lessgtr}$ and $\tilde{B}_{k_0} = \tilde{\gamma}_{k_0}$ is an arbitrary constant. In fact, since one of the upper parameters of the Gauss function is zero, the nonnormalized solution is simply

$$f_{k_0}(\Theta) = C_{k_0,C}^{k_1,k_2} |\cos \Theta_C|^{-2k_1+3/2} |\sin \Theta_C|^{-2k_2+3/2}, \tag{10.11}$$

valid in the three charts $C = H_<, P, H_>$ with Θ_C as in (6.13). The ratio of the normalization coefficients $C_{k_0,C}^{k_1,k_2}$ in each pair of "adjoining" charts may be found through requiring that it be orthogonal to any other f_k, $k \in D$. This requirement leads to

$$C_{k_0,H_>}/C_{k_0,P} = (\beta_k/\tilde{\beta}_k)^{1/2}, \quad C_{k_0,H_<}/C_{k_0,P} = (\gamma_k/\tilde{\gamma}_k)^{1/2}, \tag{10.12}$$

which in turn demands that $\beta_k/\tilde{\beta}_k$, $k = \epsilon + n$, $n \in Z^+$, be independent of $k - \epsilon$, or a periodic function of k with period unity. This property is satisfied by (10.6). The norm of the

exceptional-series state may not be calculated through (10.5) since the process $l \to k_0$ is invalid here [it would give a fictitious infinite norm to the exceptional state (10.11)]. It may be obtained directly, however. Once the normalized solution is found, the rest of the program follows.

The CGC's for the coupling $E \times E \to E$ are thus found:

$$C\begin{pmatrix}\epsilon_1,k_1, & \epsilon_2,k_2;\epsilon,k_0\\ \tau_1,\rho_1, & \tau_2,\rho_2; +1,\rho\end{pmatrix} = \delta(\tau_1\rho_1^2/2 + \tau_2\rho_2^2/2 - \rho^2/2)$$
$$\times c_{k_0,E}^{k_1,k_2}[\sin\pi(k_1 - \tau_1\epsilon_1)\sin\pi(k_2 - \tau_2\epsilon_2)]^{1/2}$$
$$\times \rho_1^{-2k_1+1}\rho_2^{-2k_2+1}\rho^{2k_0-1}, \tag{10.13a}$$

where we have written an expression valid for all three charts; the normalization coefficient is

$$c_{k_0,E}^{k_1,k_2} = (2\pi)^{1/2}[\Gamma(-2k_1+2)\Gamma(-2k_2+2)\Gamma(2k_0-1)$$
$$\times\{\sin\pi(2k_1-1)\sin\pi(k_1-\epsilon_1)\sin\pi(k_2+\epsilon_2)$$
$$+\sin\pi(2k_2-1)\sin\pi(k_1+\epsilon_1)\sin\pi(k_2-\epsilon_2)$$
$$+\sin\pi(2k_0-1)\sin\pi(k_1-\epsilon_1)\sin\pi(k_2-\epsilon_2)\}]^{-1/2}. \tag{10.13b}$$

For total $\tau = -1$, (6.21) may be used.

10.4: The last case to be analyzed pertains to the coupling of two continuous-series SAIR's to SAIR's in the continuous series. Corresponding to each eigenvalue $-(2k-1)^2 > 0$, there are two independent generalized solutions to the eigenvalue problem. The solution functions f_k may be given the following forms in each of the three charts:

$$f_k^{H_>}(\theta) = G_{k,\varphi}^{>} w_{1(\infty)}^{k_1,k_2,k}(\theta) + \tilde{G}_{k,\varphi}^{>} w_{2(\infty)}^{k_1,k_2,k}(\theta)$$
$$= \alpha_> D_{k,\varphi} w_{1(0)}^{k_1,k_2,k}(\theta) + \alpha_>^{-1}\tilde{D}_{k,\varphi} w_{2(\infty)}^{k_1,k_2,k}(\theta), \tag{10.14a}$$

$$f_k^{P}(\theta) = D_{k,\varphi} w_{1(0)}^{k_1,k_2,k}(\theta) + \tilde{D}_{k,\varphi} w_{2(0)}^{k_1,k_2,k}(\theta)$$
$$= \varphi_k w_{1(1)}^{k_1,k_2,k}(\theta) + \varphi_k^{-1} w_{2(1)}^{k_1,k_2,k}(\theta), \tag{10.14b}$$

$$f_k^{H_<}(\theta) = \alpha_< \varphi_k w_{1(0)}^{k_2,k_1,k}(\theta) + \alpha_<^{-1}\varphi_k^{-1} w_{2(0)}^{k_2,k_1,k}(\theta),$$
$$= G_{k,\varphi}^{<} w_{1(\infty)}^{k_2,k_1,k}(\theta) + \tilde{G}_{k,\varphi}^{<} w_{2(\infty)}^{k_2,k_1,k}(\theta). \tag{10.14c}$$

Our starting point will be the "common" boundary between the $H_<$- and P-charts in Fig. 6, where we propose $f_k^P(\theta)$ in (9.14b) to be a linear combination of the two solutions $w_{n(1)}^{k_1,k_2,k}(\theta)$, $n = 1,2$, with a free parameter φ_k. The choice of real solutions requires that $|\varphi_k| = 1$ when $k_1 \in C$ and $\varphi_k = \varphi_k^*$ when $k_1 \in E$. All other coefficients in (9.14) except the α's are to depend on the choice of φ_k. When $k_1 \in E$ is such that $\pm\epsilon_1 \to k_1$, the $D \times \mathscr{C}$ coupling of the last section will be recovered in the limit $\varphi_k \to \infty$ (the overall normalization constant will ensure that only the $w_{2(1)}^k$ term vanishes, with no other singularity present). The $D_{k,\varphi}$ and $\tilde{D}_{k,\varphi}$ are uniquely determined in terms of φ_k through the $z \leftrightarrow 1-z$ transformations of the Gauss functions as in (9.3) and its $k_1 \leftrightarrow 1-k_1$ replacement. Given $f_k^P(\theta)$ at $\theta = 0$ and $\pi/2$, the forms (10.14a)–(10.14c) of $f_k^{H_>}(\theta)$ and $F_k^{H_<}(\theta)$ at $f_k^{H_<}(\theta)$ at $\theta_{H_>} = 0$ and $\theta_{H_<} = 0$ are determined up to coefficients $\alpha_>$ and $\alpha_<$ If the boundary Wronskians of any two solutions f_k and f_l, $k,l \in C$ are to vanish, the α's must be independent of k and l. Their role is thus the analog of the α introduced in (9.9b). When $k_1 \in C$, $|\alpha_<| = 1$, while when $k_1 \in E$, $\alpha_< = \alpha_>^*$; similar conditions hold for $\alpha_>$ in terms of k_2. Now, orthogonality of f_k, $k \in C$ to f_l, $l \in D$, requires that $\alpha_> = (\tilde{\beta}_k/\beta_k)^{1/2}$ and $\alpha_< = (\gamma_k/\gamma_k)^{1/2}$, and hence the ratios $\tilde{\beta}_k/\beta_k$, γ_k/γ_k must be independent of k (when $k = \epsilon + n$, $n \in Z^+$). This condition is compatible with (10.12) and satisfied by (10.6), which also exhibits the corresponding reality properties. Orthogonality to the exceptional state f_{k_0} in (10.11) is automatically assured.

The last constants to be determined in terms of φ_k are the coefficients of the $w_{n(\infty)}^k$. The $z \leftrightarrow 1/z$ transformation of the Gauss functions—the inverse of (9.4) and its $k \leftrightarrow 1-k$ replacement—yields

$$G_{k,\varphi}^{>} = [\sin\pi(k_2+\epsilon_2)\sin\pi(k_2-\epsilon_2)]^{-1/2}$$
$$\times\{\sin\pi[-(k_1-\epsilon_1)+(k-\epsilon)]C(k_1,k_2,k)\varphi_k$$
$$+\sin\pi[-(k_1+\epsilon_1)-(k-\epsilon)]C(1-k_1,k_2,k)\varphi_k^{-1}\}, \tag{10.15a}$$

$$\tilde{G}_{k,\varphi}^{>} = G_{1-k,\varphi}^{>} = (G_{k,\varphi}^{>})^*, \tag{10.15b}$$

$$G_{k,\varphi}^{<} = [\sin\pi(k_1+\epsilon_1)\sin\pi(k_1-\epsilon_1)]^{-1/2}$$
$$\times[\sin\pi(k_1-\epsilon_1)C(k_1,k_2,k)\varphi_k$$
$$+\sin\pi(k_1+\epsilon_1)C(1-k_1,k_2,k)\varphi_k^{-1}], \tag{10.16a}$$

$$\tilde{G}_{k,\varphi}^{<} = G_{1-k,\varphi}^{<} = (G_{k,\varphi}^{<})^*, \tag{10.16b}$$

where

$$C(k_1,k_2,k) = \Gamma(2k_1)\Gamma(2k-1)/\Gamma(k_1-k_2+k)$$
$$\times\Gamma(k_1+k_2+k-1). \tag{10.17}$$

The equalities (10.15b) and (10.16b) [compare with (9.9a)] are the ones which insure that two solutions $f_{k,\varphi}$, $f_{l,\varphi}$, $k,l \in C$ may be subject to Dirac normalization though their cross-Wronskians at $\theta_{H_>} \to \infty$ in the manner of (4.9). The overall normalization of (10.14) will then be

$$c_{k,\varphi} = [2\pi(|G_{k,\varphi}^{>}|^2 + |G_{k,\varphi}^{<}|^2)]^{-1/2}. \tag{10.18}$$

Similarly, two solutions $f_{k,\varphi}$ and $f_{k,\psi}$ will be orthogonal when the two cross-Wronskians cancel. This happens when φ_k and ψ_k are such that

$$G_{k,\varphi}^{>}(G_{k,\psi}^{>})^* + (G_{k,\varphi}^{<})^* G_{k,\psi}^{<} = 0. \tag{10.19a}$$

A special choice of mutually orthogonal solutions, labeled by φ_+ and φ_-, may be built demanding

$$G_{k,\varphi_\pm}^{<} = \pm(G_{k,\varphi_\pm}^{>})^*. \tag{10.19b}$$

When the conjugation properties in (10.15) and (10.16) are used, (10.19b) yields an algebraic expression for $(\varphi_\pm)^2$. Alternatively, (10.19a) embodies the Schmidt orthogonalization process for generalized functions whereby a $f_{k,\psi}$ may be found which is orthogonal to any given $f_{k,\phi}$. For $k_1 \in E$, finally, the choice of $\varphi \to \infty$ yields a preferred $\mathscr{C} \times \mathscr{C} \to C$ CGC coefficient, which upon $\pm\epsilon_1 \to k_1$, yields the $D \times \mathscr{C} \to C$ CGC's seen in the last section.

Unfortunately, when (10.15)–(10.19) are substituted in (10.4), no significant algebraic reductions seem to take place in the final expressions, which would merit their explicit display. For the $\mathscr{C} \times \mathscr{C} \to C$ coupling we may thus write

$$C^{\varphi}_{>}\begin{pmatrix}\epsilon_1,k_1, & \epsilon_2,k_2; & \epsilon,k\\ 1+,\rho_1, & -1,\rho_2; & +1,\rho\end{pmatrix}=\delta(\rho_1^2/2-\rho_2^2/2-\rho^2/2)c_{k,\varphi}$$
$$\times\left\{G^{>}_{k,\varphi}\rho_1^{2k_1-1}\rho_2^{-2k_1+2k-1}\rho^{-2k+1}F\left[\begin{matrix}k_1+k_2-k,k_1-k_2-k+1\\ 2-2k\end{matrix};-\rho^2/\rho_2^2\right]+(k\leftrightarrow 1-k)\right\}, \tag{10.20a}$$

$$C^{\varphi}\begin{pmatrix}\epsilon_1,k_1, & \epsilon_2,k_2; & \epsilon,k\\ +1,\rho_1, & +1,\rho_2; & +1,\rho\end{pmatrix}=\delta(\rho_1^2/2+\rho_2^2/2-\rho^2/2)c_{k,\varphi}$$
$$\times\left\{\varphi\left(\rho_1^{2k_1-1}\rho_2^{2k_2-1}\rho^{-2k_1-2k_2+1}F\left[\begin{matrix}k_1+k_2-k,k_1+k_2+k-1\\ 2k_1\end{matrix};\rho^2/\rho_1^2\right]\right)+\varphi^{-1}(k_1\leftrightarrow 1-k_1)\right\}, \tag{10.20b}$$

$$C^{\varphi}_{<}\begin{pmatrix}\epsilon_1,k_1, & \epsilon_2,k_2; & \epsilon,k\\ -1,\rho_1, & +1,\rho_2; & +1,\rho\end{pmatrix}=\delta(-\rho_1^2/2+\rho_2^2/2-\rho^2/2)c_{k,\varphi}$$
$$\times\left\{G^{<}_{k,\varphi}\rho_1^{-2k_2+2k-1}\rho_2^{2k_2-1}\rho^{-2k+1}F\left[\begin{matrix}k_1+k_2-k,-k_1+k_2-k+1\\ 2-2k\end{matrix};-\rho^2/\rho_1^2\right]+(k\leftrightarrow 1-k)\right\}. \tag{10.20c}$$

For $\tau=-1$, (6.21) may be used.

XI. CONCLUDING REMARKS

The explicit construction of the Clebsch–Gordan coefficients for an algebra is but one of a set of related problems whose complete elucidation for so(2,1) is of interest in mathematical physics. This algebra is, after all, the simplest of all noncompact semisimple Lie algebras. The symmetry, composition, and asymptotic properties of the so(3) CGC's have been fruitfully exploited, but their so(2,1) counterparts have not yet received a comparable coverage. Composition properties such as (1.1) entail special-function relations between confluent and Gauss hypergeometric functions; the Plancherel measure[22] and the SO(2,1) UIR matrix elements[23] in the parabolic and other bases are known, and now the CGC's are available. The same remarks apply for the orthogonality and completeness relations for the CGC's, as well as a deeper study of their analyticity properties[3] with respect to the SAIR indices k_1,k_2,k, extended to indecomposable, finite-dimensional, and other non-self-adjoint representations of the algebra.

CGC's in bases other than the parabolic basis may be computed and compared with the existing results. This involves integrating the coefficients with the overlap functions between the iso(1) basis used here, and the so(1,1) or so(2) bases.[23] The former requires a triple Mellin transform of our results over ρ_1,ρ_2, and ρ and summation over the range of τ's to compare with the results of Mukunda and Radhakrishnan[7]; the latter a triple Laguerre and/or Whittaker transform to compare with Holman and Biedenharn's work.[4] In relation with the former—a still practical calculation—one may obtain independently the matrix elements of SO(3,1) and SO(2,2) in various bases.

Perhaps the nearest task of interest is the analog of Sec. V, the study of all common self-adjoint extensions of a second-order differential operator algebra, as applied to the N-dimensional symplectic algebra sp($2N,R$). The oscillator representation of the latter is well known,[12] and certain special cases of the "radial/hyperbolic" reductions sp($2rs$) $\supset$ Sp($2r$) + so($s-t,t$) have been subject to scrutiny,[24] in particular sp(4) $\approx$ so(3,2). Finally, one may realistically hope that the CG and representation problems for the four-dimensional Lorentz, Poincaré, and conformal algebras may simplify in their analog of the parabolic basis, as it did here, for so(2,1).

ACKNOWLEDGMENTS

We would like to thank Dr. Alberto Alonso y Coria and Dr. Ricardo Weder (IIMAS—UNAM) for their interest in our work, as well as Dr. H. Kalb, of Universität Darmstadt, for a crucial illuminating discussion on the properties of strongly singular potentials.

APPENDIX

The self-adjoint irreducible representations of the three-dimensional Lorentz algebra so(2,1), with generators J_1, J_2, J_0 satisfying the commutation relations (2.1f), may be classified[1,25] through the eigenvalue q of the Casimir operator $Q=J_1^2+J_2^2-J_0^2$, and either a "multivaluation" index $\epsilon\in(-\frac{1}{2},\frac{1}{2}]$ or a sign $\tau=\pm 1$. The latter two indicate the common self-adjoint extension of the algebra generators as detailed in Sec. V; ϵ is given by the spectrum $\{\mu\}$ of the elliptic subalgebra generator J_0, modulo unity. When unique, τ specifies the sign of the parabolic subalgebra generator $J_-=J_0-J_1$. The representations are conveniently labeled also by a parameter k which relates to q through $q=k(1-k)$. The equivalence under $k\leftrightarrow 1-k$ is used in the $\mathscr{C}$-series (below) to reduce its range to $\mathrm{Re}k\geqslant\frac{1}{2}$.

The classification of the SAIR's of so(2,1) is as follows [$R^+=[0,\infty)$, $Z^+=\{0,1,2,\cdots\}$]:

Continuous series ($\mathscr{C}$):

C: Nonexceptional (C^{ϵ}_{q}):

$q\geqslant\frac{1}{4}$ [i.e., $k=(1+i\kappa)/2$, $\kappa\in R^+$], $\epsilon\in(1-\frac{1}{2},\frac{1}{2}]$

with the exception of $q=\frac{1}{4}$ [i.e., $k=\frac{1}{2}$, $\kappa=0$], $\epsilon=\frac{1}{2}$.

E: Exceptional (C^{ϵ}_{q}):

$0<q<\frac{1}{4}$ [i.e., $k=(1+\kappa)/2$, $\kappa\in(0,1)$], $|\epsilon|<1-k$.

In both subcases: $\mu\in\{\epsilon+n, n\in Z\}$, $\tau\in\{-1,+1\}$.

Discrete series ($\mathscr{D}$)

D^+: *Positive discrete series* (D_k^+):

$k>0$ [i.e., $q\leqslant\frac{1}{4}$], $\epsilon\equiv k \pmod 1$,

$\mu\in\{k+n, n\in Z^+\}$, $\tau=+1$.

D^-: *Negative discrete series* (D_k^-):

$k>0$ [i.e., $q\leqslant\frac{1}{4}$], $\epsilon\equiv -k \pmod 1$,

$\mu\in\{-k-n, n\in Z^+\}$, $\tau=-1$.

The $k\leftrightarrow 1-k$ symmetry can be upheld in the exceptional interval -$\mathscr{D}$, $0<k<1$ if we ascribe $\epsilon=k\in(0,\frac{1}{2}]$ to $1-k\in[\frac{1}{2},1)$ and keep $0<\epsilon\leqslant\frac{1}{2}$, while for $k\in(\frac{1}{2},1]$ we take $0>\epsilon=1-k>-\frac{1}{2}$.

The Clebsch–Gordan series[2,4] are written below. We use the following conventions:

(i) All sums are direct and range over integer-spaced k's.

(ii) Direct integrals, as written, do not exhibit the Plancherel measure.[22]

(iii) In all cases $\epsilon=\epsilon_1+\epsilon_2 \pmod 1$, with $\epsilon_j\equiv\pm k_j \pmod 1$ for $k_j\in\mathscr{D}$.

(iv) The numerals in brackets indicate the formulae in this article where the corresponding CGC's are given.

$\mathscr{D}\times\mathscr{D}$:

$$D_{k_1}^{\pm}\times D_{k_2}^{\pm}=\sum_{k=k_1+k_2}^{\infty} D_k^{\pm}, \qquad [(7.1)]$$

$$D_{k_1}^{\pm}\times D_{k_2}^{\mp}=\sum_{1/2<k}^{|k_1-k_2|} D_k^{\mathrm{sgn}(k_1-k_2)}+\int_{k\in C} C_q^{\epsilon} \quad [(8.4),(8.1)]$$
$$+(D_{1/2}^{\mathrm{sgn}(k_1-k_2)} \text{ when } |k_1-k_2|=\tfrac{1}{2}); \qquad [(8.1)]$$

$\mathscr{D}\times\mathscr{C}$:

$$D_{k_1}^{\pm}\times C_{q_2}^{\epsilon_2}=\sum_{k=\epsilon}^{\infty} D_k^{\pm}+\int_{k\in C} C_q^{\epsilon}; \qquad [(9.7),(9.1)\text{–}(9.8)]$$

$\mathscr{C}\times\mathscr{C}$:

$$C_{q_1}^{\epsilon_1}\times C_{q_2}^{\epsilon_2}=\sum_{k=\epsilon}^{\infty} D_k^{+}+\sum_{k=\epsilon}^{\infty} D_k^{-}+2\int_{k\in C} C_q^{\epsilon}$$
$$[(10.7)\text{–}(10.9),(10.20)]$$
$$+(C_q^{\epsilon}[k=k_1+k_2-1] \quad \text{for } k_1,k_2,k\in E). \qquad [(10.13)]$$

[1] V. Bargmann, Ann. Math. **48**, 568 (1947).
[2] L. Pukánszky, Trans. Am. Math. Soc. **100**, 116 (1961).
[3] W. J. Holman and L. C. Biedenharn, Ann. Phys. (N.Y). **39**, 1 (1966).
[4] W. J. Holman and L. C. Biedenharn, Ann. Phys. (N.Y.) **47**, 205 (1968).
[5] I. Ferretti and M. Verde, Nuovo Cimento **55**, 110 (1968); M. Verde, *Proceedings of the Mendeleevian Conference*, Torino, 1969 (Torino Academy of Science, Torino, Italy, 1971), p. 305.
[6] K. H. Wang, J. Math. Phys. **11**, 2077 (1970).
[7] N. Mukunda and B. Radhakrishnan, J. Math. Phys. **15**, 1320, 1322, 1643, 1656 (1974).
[8] M. Andrews and J. Gunson, J. Math. Phys. **5**, 1391 (1964); S. S. Sannikov, Dokl. Akad. Nauk SSSR **171**, 1058 (1967) [Sov. Phys. Dokl. **11**, 1045 (1967)]; H. Ui, Ann. Phys. (N.Y.) **49**, 69 (1969); A. O. Barut and R. Wilson, J. Math. Phys. **17**, 900 (1976); E. Chaćon, D. Levi, and M. Moshinsky, J. Math. Phys. **17**, 1919 (1976); S. D. Majumdar, J. Math. Phys. **17**, 193 (1976); D. Basu and S. D. Majumdar, J. Math. Phys. **20**, 492 (1979); D. Basu, "The Master Analytic Function and the Lorentz Group," Kinam (to be published).
[9] J. L. Burchnall and T. W. Chaundy, Proc. London Math. Soc. **50**, 56 (1944).
[10] J. Schwinger, AEC Report, 1952 (unpublished), reprinted in *Quantum Theory of Angular Momentum*, edited by L. C. Biedenharn and H. van Dam (Academic, New York, 1965); A. Malkin and V. I. Man'ko, Pisma Zh. Eksp. Teor. Fiz. **2**, 230 (1965) [JETP Lett. **2**, 146 (1966)]; A. O. Barut and A. Bohm, J. Math. Phys. **11**, 2938 (1970).
[11] A. Weil, Acta Math. **11**, 143 (1963).
[12] M. Moshinsky and C. Quesne, J. Math. Phys. **12**, 1772, 1780 (1971); M. Moshinsky, SIAM J. Appl. Math. **25**, 193 (1973).
[13] (a,b) K. B. Wolf, J. Math. Phys. **15**, 1295, 2102 (1974); (c) C. P. Boyer and K. B. Wolf, J. Math. Phys. **16**, 1493 (1975); (d) K. B. Wolf, J. Math. Phys. **21**, 680 (1980).
[14] K. B. Wolf, *Integral Transforms in Science and Engineering* (Plenum, New York, 1979).
[15] N. Mukunda and B. Radhakrishnan, J. Math. Phys. **14**, 254 (1973).
[16] G. Pöschl and E. Teller, Z. Phys. **83**, 143 (1933).
[17] M. Rosen and P. M. Morse, Phys. Rev. **42**, 210 (1932); W. Lotmar, Z. Phys. **93**, 528 (1935); L. Infeld and T. E. Hull, Rev. Mod. Phys. **23**, 21 (1951), Sec. 4.8.
[18] M. Reed and B. Simon, *Methods of Modern Mathematical Physics* (Academic, New York, 1975), Vol. 2.
[19] M. Abramowitz and I. A. Stegun (Eds.), *Handbook of Mathematical Functions* (National Bureau of Standards, Washington, D.C., 1964).
[20] K. Meetz, Nuovo Cimento **34**, 690 (1964).
[21] I. S. Gradshteyn and I. M. Ryzhik, *Tables of Integrals, Sums and Products* (Academic, New York, 1965).
[22] L. Pukánszky, Math. Ann. **156**, 96 (1964).
[23] D. Basu and K. B. Wolf, "The Unitary Irreducible Representations of SL (2,R) in All Subgroup Decompositions," J. Math. Phys. **23**, 189 (1982).
[24] M. Moshinsky, T. H. Seligman, and K. B. Wolf, J. Math. Phys. **13**, 901 (1972); P. Kramer, M. Moshinsky, and T. H. Seligman, in *Group Theory and Its Applications*, Vol. III, edited by E. M. Loebl (Academic, New York, 1975); M. Kashiwara and M. Vergne, Invest. Math. **44**, 1 (1978).
[25] P. J. Sally, Jr., Bull. Am. Math. Soc. **72**, 269 (1966).